LA-UR-13-26804
Approved for public release; distribution is unlimited.

Title: Influence of relative permeability parameters on CO2 injectivity

Author(s): Yoshida, Nozomu
Stauffer, Philip H.

Intended for: Report

Issued: 2013-08-29

Influence of relative permeability parameters on CO2 injectivity

Nozomu Yoshida, Philip H. Stauffer

Earth and Environmental Sciences Division

Computational Earth Sciences Group EES-16

August 2013

1 Introduction

1.1 Background and literature review

Relative permeability between brine and carbon dioxide (CO_2) is one of the crucial parameters on the injectivity when CO_2 is injected into the deep saline aquifer for the geologic CO_2 sequestration. In order to quantify the relative permeability relationship between brine and CO_2, several researchers conducted experimental works. Muller (2010) summarized the literatures on the experimental works by Perrin et al. (2009), Bennion and Bachu (2006), Chalbaud et al. (2007), Egermann et al. (2006) and Dria et al. (1993). Especially, Bennion and Bachu examined the relative permeability characteristics for supercritical CO_2 and brine system in several rock types (e.g. intergranular sandstone, carbonate, shale and anhydrite) publishing their measurement data (Bennion and Bachu 2005, 2007, 2008, 2009). In their work (Bennion and Bachu 2008), they showed the best-fitted parameter values in the extended Corey's relative permeability model through regression analysis, and their results are used in some simulation works of the CO_2 injection into the saline aquifers (Azizi and Cinar 2013). In addition, Levine (2011) performed experimental work mainly to measure endpoint relative permeability rather than the entire relative permeability curve, paying special attention to achieving residual saturation at the core inlet. This work incorporated the capillary end effects to obtain accurate values of endpoint relative permeability. Recently, Mohamed and Nasr-El-Din (2013) performed laboratory and modeling studies on the fluid-carbonate rock interaction and the relative permeability curves, and they confirmed their experimental results are consistent with the results given by Bennion and Bachu (2008).

Through these experimental works, it is confirmed that the relative permeability depends on a variety of parameters like pressure, temperature, interfacial tension between brine and CO_2, bine salinity, wettability of rocks, absolute permeability, porosity, hysteresis and even the experimental procedure (e.g. steady state or unsteady state experiment) (Bennion and Bachu 2005, 2007, 2008, 2009; Doughty 2007; Juanes et al. 2006; Liu et al. 2010; Mohamed and Nasr-El-Din 2013; Muller 2010). Therefore, the relative permeability curve is regarded as one of the possible uncertain variables in the numerical simulation of the geologic CO_2 sequestration, though usually only one set of relative permeability curve is used in the drainage process.

Comparing to CO_2 injection works for the enhanced oil recovery, usually, detailed information about the reservoir where the CO_2 is injected is not available in the geologic CO_2 sequestration (Stauffer et al. 2006). In order to quantify the uncertainty in the geologic sequestration, uncertainty quantification in the geologic heterogeneity on the injectivity and storage capacity has been examined by several works (Deng et al. 2012; Heath et al. 2012). But, the uncertainty of the injectivity in CO_2 sequestration due to the relative permeability has not been examined intensively so far.

1.2 Objective and approach

In this report, we perform uncertainty quantification on the injectivity due to the variation of relative permeability curves and explain the source of the uncertainty through the interpretation of each parameter in the relative permeability model. We use the extended Corey's model as used in Bennion and Bachu (2008) and Levine (2011). This model has mainly four parameters in the drainage process; residual brine saturation, brine exponent, CO_2 exponent and endpoint CO_2 relative permeability, and the effects of

variations in these parameters on the injectivity are examined through a sensitivity study. The uncertainty quantification and the interpretation of the reasons for the uncertainty may provide insights on the implementation of the relative permeability module for the reduced-order model of CO_2 sequestration (CO2-PENS).

In the following chapters, at first, we perform a preliminary study of the variation of injectivity using the results given by the core-flooding experiments and regression analysis (Bennion and Bachu, 2008). We try to find out influential parameters on the injectivity in the relative permeability model. Next, the parameter sensitivity study is performed using the same data set except some rock types (shale and anhydrite). The statistical parameter values and the probability distributions are assumed by the data. Only is one target parameter value changed with the others constant to run simulations, and the results are compared to base case results to quantify the sensitivity of injectivity on the target parameter. Finally, a Monte Carlo simulation is performed to calibrate the results given by the parameter sensitivity study and to quantify the uncertainty in the target problem due to the variation of the relative permeability curve. In this part, the reasons for the uncertainty are explained utilizing the results by the sensitivity study. We will sum up this report with some discussions on the results and conclusions given by the simulations with some implications for the reduced-order model.

2 Model Setup

2.1 Model description

In this report, we use a 2-D radial, homogeneous and isotropic saline reservoir model. The reservoir is overlain by a cap rock and underlain by a bed rock formation. The reservoir is initially filled by fresh water (no salinity) and the mutual solubility between the CO_2 and water is ignored. The CO_2 is injected into the reservoir with the constant injection pressure (16.5 MPa), and the injection is performed for 4 years. The temperatures at the upper boundary and lower boundary are set to constant. The other parameters used in the simulation are summarized in **Table 1**, and the schematics of the model geometry are shown in **Fig. 1**. The numerical flow and thermal simulation is performed using FEHM with the grid system shown in **Fig. 2**. This is the logarithmic spacing to the r-direction and the uniform spacing (0.5 m) to the z-direction. The total number of node is 40401.

TABLE 1 – RESERVOIR PARAMETERS

Parameter	Value
Cap/bed rock permeability, m^2	10^{-19}
Saline reservoir permeability, m^2	10^{-13}
Porosity, -	0.1
Initial reservoir pressure, MPa	11
Initial reservoir temperature, ℃	36
Reservoir thickness, m	20

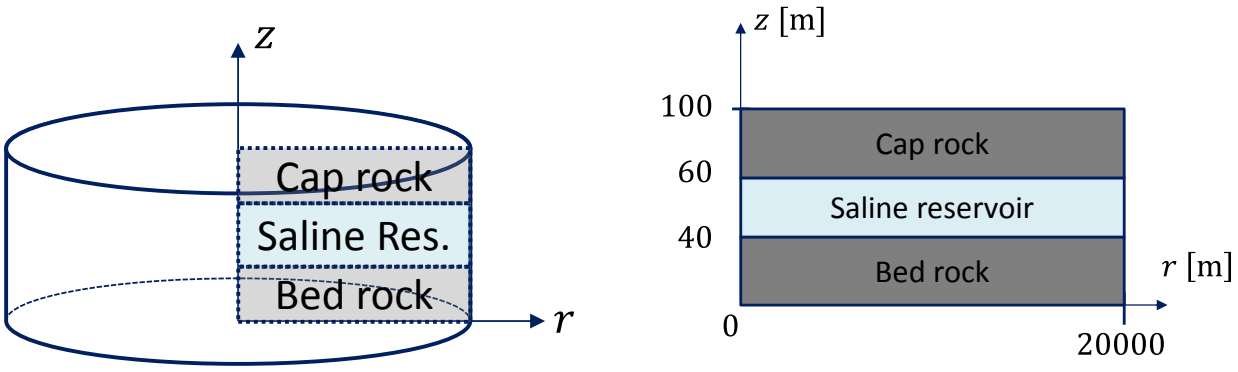

(a) Reservoir Geometry (Cylindrical reservoir) (b) Cross section of the reservoir

Fig. 1 – Schematics of reservoir geometry

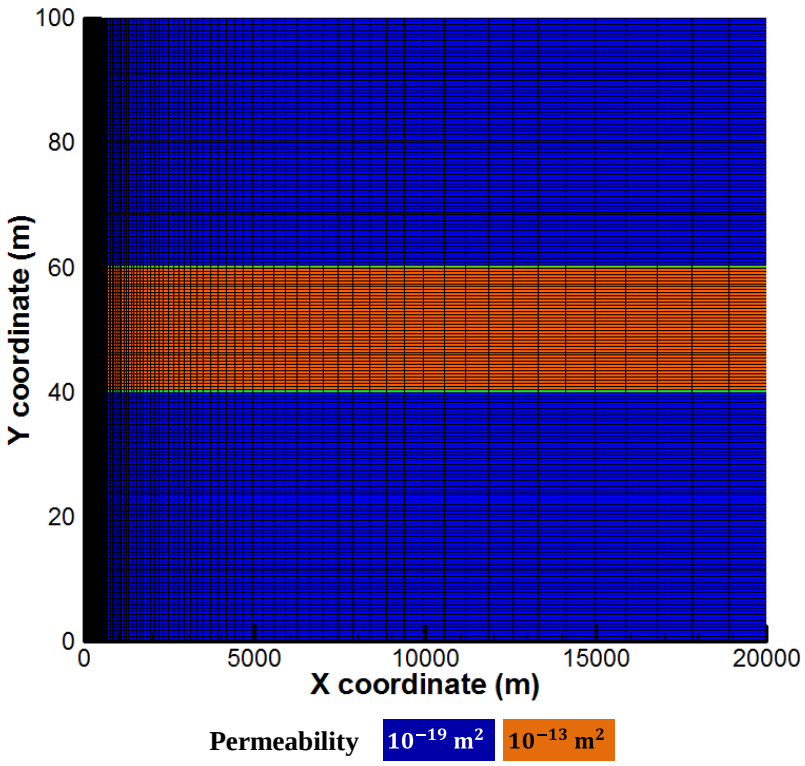

Fig. 2 – Numerical mesh design for the target problem with absolute permeability

The capillary pressure model used in this work is van Genuchten model (1980) in the form of

$$P_c = P_0\left[(S^*)^{-1/\lambda} - 1\right]^{1-\lambda} \quad \text{.....(1)}$$

where λ is the pore size distribution index, and S^* is given by

$$S^* = \frac{S_{brine} - S_{brine,ir}}{1 - S_{brine,ir}}, \quad \text{.....(2)}$$

and $S_{brine,ir}$ is the irreducible brine saturation. Input parameter values of this model are summarized in **Table 2** (these are taken after the benchmarking problem #3 in Pruess et al. (2002)). The capillary pressure curve is not changed in this work. The relative permeability model used in this work is described in the next section.

TABLE 2 – INPUT PARAMETERS FOR CAPILLARY PRESSURE MODEL

Parameter	Value
P_0, kPa	19.61
$S_{brine,ir}$, -	0
λ, -	0.457

2.2 Relative permeability model

Relative permeability model used in this report is an extension of the Corey's model, which can be expressed in the general form

$$k_{r,CO2} = k^0_{r,CO2}\left(\frac{S_{CO2}-S_{CO2,ir}}{1-S_{CO2,ir}-S_{brine,ir}}\right)^m \quad \text{.....(3)}$$

and

$$k_{r,brine} = k^0_{r,brine}\left(\frac{S_{brine}-S_{brine,ir}}{1-S_{CO2,ir}-S_{brine,ir}}\right)^n \quad \text{.....(4)}$$

where $k_{r,CO2}$ and $k_{r,brine}$ are the relative permeability of the CO_2 and brine, $k^0_{r,CO2}$ and $k^0_{r,brine}$ are the endpoint relative permeability of CO_2 and brine, S_{CO2} and S_{brine} are the saturation of CO_2 and brine, $S_{CO2,ir}$ and $S_{brine,ir}$ are the residual or irreducible CO_2 and brine saturations, and m and n are the exponents of the CO_2 and brine. Because these results were given for the drainage process, the values of $k^0_{r,brine}$ and $S_{CO2,ir}$ are set to 1.0 and 0.0, respectively. Therefore, the relative permeability model is simplified as

$$k_{r,CO2} = k^0_{r,CO2}\left(\frac{S_{CO2}}{1-S_{brine,ir}}\right)^m \quad \text{.....(5)}$$

and

$$k_{r,brine} = \left(\frac{S_{brine}-S_{brine,ir}}{1-S_{brine,ir}}\right)^n. \quad \text{.....(6)}$$

The data given by the core-flooding experiments and the regression analysis (Bennion and Bachu, 2005; 2008) is used as the input data of the extended Corey's model. They did the measurements and the analysis on the variety of rock type and permeability range. The experimental conditions and results are summarized in **Table 3** and **Table 4**, respectively. The calibration of the regression analysis using the extended Corey's model with the measured data was performed and the results are summarized in the appendix (**Fig. A.1**). In addition, the relative permeability curves by the data are also shown in the appendix (**Fig. A.2**).

TABLE 3 – EXPERIMENTAL CONDITION IN BENNION AND BACHU (2005, 2008)

Formation Unit	Lithology	Porosity, %	Pressure, MPa	Temperature, ℃	Salinity, mg/L
Colorado	Shale	4.4	20.00	43	27,100
Cardium #1	Sandstone	15.3	20.00	43	27,100
Cardium #2	Sandstone	16.1	20.00	43	27,100
Viking #1	Sandstone	12.5	8.60	35	28,300
Viking #2	Sandstone	19.5	8.60	35	28,300
Ellerslie	Sandstone	12.6	10.90	40	94,200
Webamun #1	Carbonate	7.9	11.90	41	144,300
Webamun #2	Carbonate	14.8	11.90	41	144,300
Calmar	Shale	3.9	12.25	43	129,700
Nisku #1	Carbonate	9.7	17.40	56	136,800
Nisku #2	Carbonate	11.4	17.40	56	136,800
Cooking Lake	Carbonate	9.9	15.40	55	233,400
Basal Cambrian	Sandstone	11.7	27.00	75	248,000
Muskeg	Anhydrite	1.2	15.00	71	189,800

TABLE 4 – RELATIVE PERMEABILITY CHARACTERISTICS DURING DRAINAGE CYCLE (BENNION AND BACHU, 2008)

Rock Sample	k_{brine} at 100% saturation, md	Residual brine saturation, $S_{b,ir}$	Brine exponent	CO_2 exponent	Endpoint $k_{r,CO2}$
Colorado	0.0000788	0.605	6.5	2.6	0.0148
Cardium #1	0.356	0.197	1.3	1.7	0.526
Cardium #2	21.17	0.425	1.2	1.3	0.129
Viking #1	2.7	0.558	2.9	3.2	0.3319
Viking #2	21.72	0.423	1.7	2.8	0.2638
Ellerslie	0.376	0.659	2.1	2.2	0.1156
Webamun #1	0.018	0.595	1.4	5.6	0.5289
Webamun #2	66.98	0.569	1.4	2.1	0.1883
Calmar	0.00000294	0.638	1.3	2.5	0.1875
Nisku #1	45.92	0.33	2.8	1.1	0.1768
Nisku #2	21.02	0.492	2.7	4.6	0.0999
Cooking Lake	65.3	0.476	3.1	5.6	0.0685
Basal Cambrian	0.081	0.294	1.8	5	0.5446

2.3 Preliminary study of injectivity

As preliminary study, 14 case simulations are performed which are summarized in Table 3 and 4. The absolute permeability is assumed to be same with the brine permeability at 100% saturation shown in Table 4. The reservoir geometry and input parameters are shown in Table 1 and, in each simulation run, the relative permeability and the absolute permeability are changed to the corresponding values in table 4. The results of the preliminary study are summarized in **Fig. 3**. Fig. 3 (a) shows the amount of cumulative CO_2 injected vs. time, and the total injected CO_2 amount is linearly increasing as time passes (the injection rate is stabilized in the linearly increasing zone). Fig. 2 (b) shows the results in the logarithmic scale (y-coordinate), and this plot clarifies the lower injectivity cases. The lowest injectivity is given by the Anhydrite, and the two shale cases follow it. It is confirmed that the injectivity depends on the absolute permeability. **Fig. 4** shows the injectivity to the parameters in the relative permeability model, but it is difficult to say there is strong correlation between these variables and the injectivity. **Fig. 5** shows the injectivity to the absolute permeability (Fig. 5 (a)) and also, in Fig. 5 (b), the injectivity to the maximum CO_2 effective permeability is shown, which is defined as

$$k_{CO2,max} = k k^0_{r,CO2}, \quad \text{.....(5)}$$

where k is the absolute permeability. As we can see in Fig. 5, the injectivity has the strong relationship with the absolute permeability ($R^2 = 0.9488$), but the maximum CO_2 effective permeability shows the higher correlation coefficient to the injectivity ($R^2 = 0.9912$). **Table 5** shows the summary of the preliminary study for the absolute permeability and the maximum CO_2 effective permeability to the total injected CO_2 amount. Through this preliminary study, it is implied that the maximum CO_2 effective permeability has the dominant role in the determination of the total injectivity. This implication is to be calibrated through the parameter sensitivity study by quantifying the sensitivity to the variation of each parameter.

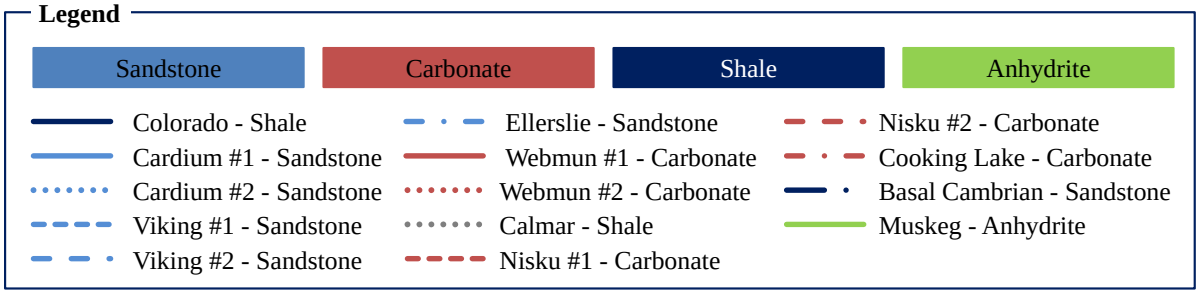

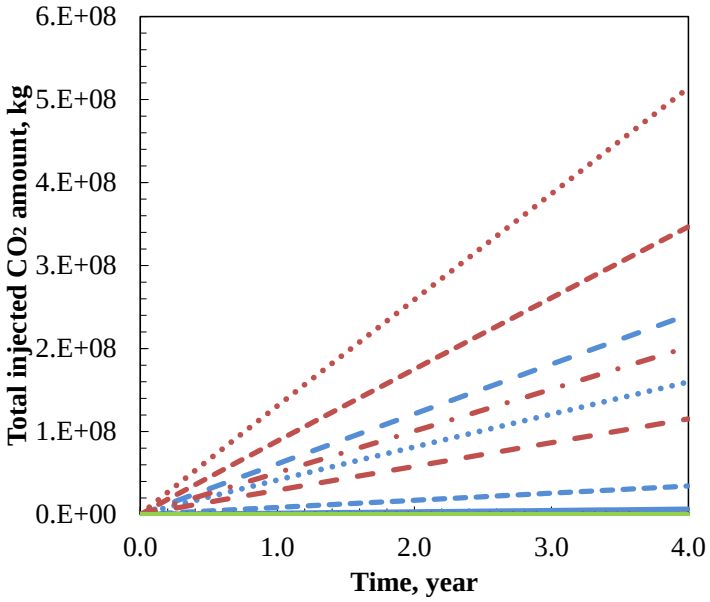

(a) Total injected CO_2 amount vs. time

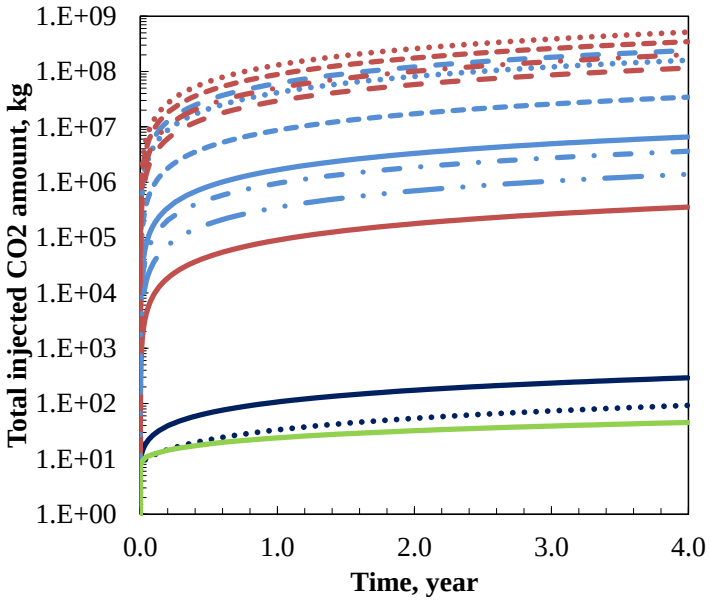

(b) Total injected CO_2 amount (log scale) vs. time

Fig. 3 – Preliminary study results of the injectivity for the 14 sample cases

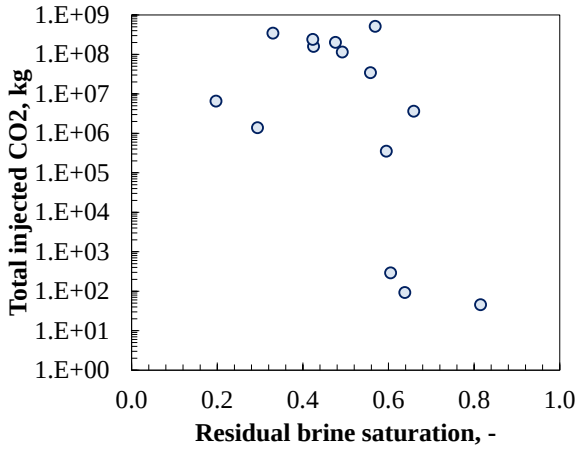

(a) Residual brine saturation

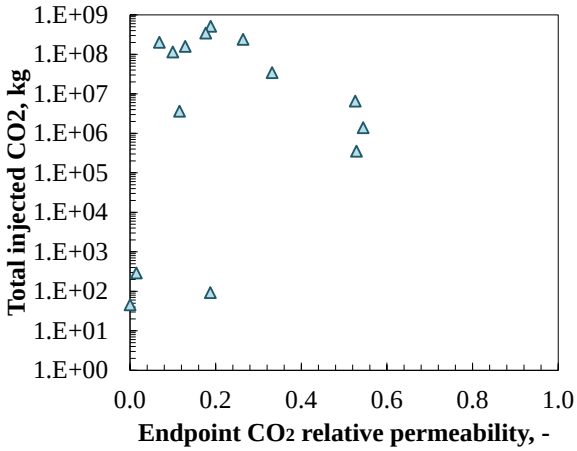

(b) Endpoint CO_2 relative permeability

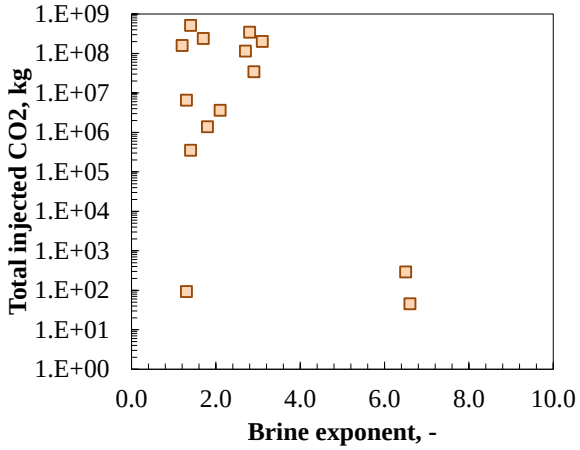

(c) Brine exponent

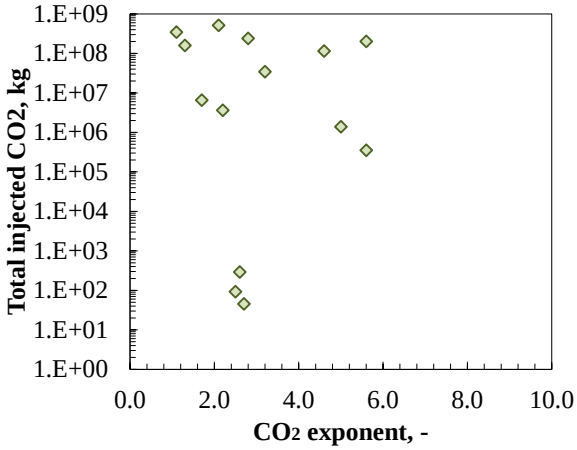

(d) CO_2 exponent

Fig. 4 – Injectivity to the parameters in the relative permeability model (preliminary study)

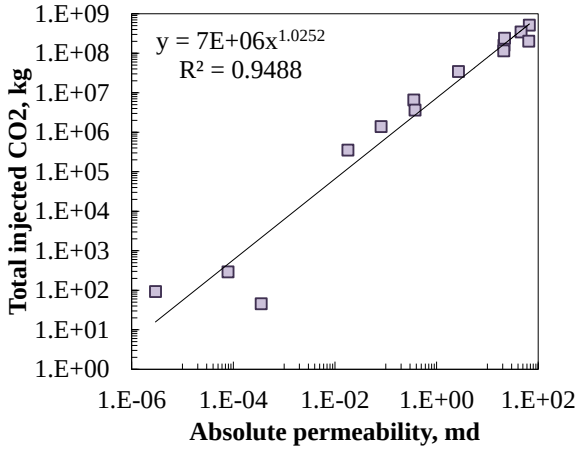

(a) Absolute permeability

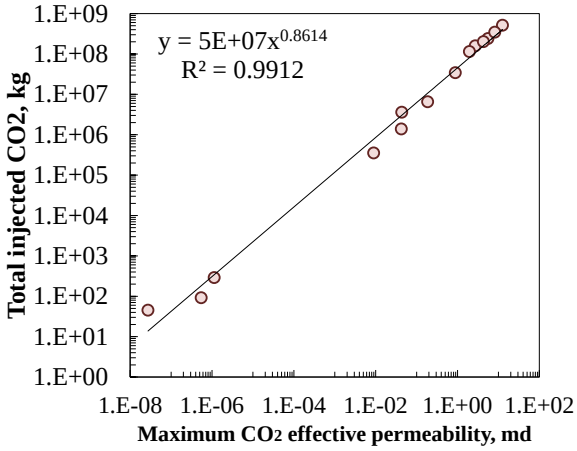

(b) Maximum CO_2 effective permeability

Fig. 5 – Injectivity to the absolute permeability and maximum CO_2 effective permeability (preliminary study)

TABLE 5 – SUMMARY OF THE PRELIMINARY STUDY				
Formation Unit	Lithology	Permeability to 100% brine, mD	Maximum CO_2 effective permeability, md	Total Injected CO_2, kg
Colorado	Shale	0.0000788	0.00000113	291
Cardium #1	Sandstone	0.356	0.186	6,558,214
Cardium #2	Sandstone	21.17	2.700	159,750,840
Viking #1	Sandstone	2.70	0.883	34,439,794
Viking #2	Sandstone	21.72	5.537	240,588,110
Ellerslie	Sandstone	0.376	0.0432	3,627,760
Webamun #1	Carbonate	0.018	0.0089	354,169
Webamun #2	Carbonate	66.98	12.55	513,720,380
Calmar	Shale	0.00000294	0.000000544	92
Nisku #1	Carbonate	45.92	8.119	346,534,420
Nisku #2	Carbonate	21.02	1.952	115,241,340
Cooking Lake	Carbonate	65.3	4.29	201,782,640
Basal Cambrian	Sandstone	0.081	0.042	1,390,364
Muskeg	Anhydrite	0.000354	0.0000000272	45

3 Parameter Sensitivity Study

3.1 Objective and approach

The objective of this sensitivity study is to determine the influential parameter on the injectivity quantitatively. In this sensitivity study, we set base values for each parameter at first. Then, one parameter value is changed and simulation is performed with no change to the others. After the simulation, the injectivity result is compared to the result by the base case, and we quantify the sensitivity to the parameter changed. This process is repeated for all of the parameters in the relative permeability model.

The base values of the parameters are estimated using the experimental results given by Bennion and Bachu (2008). They provided 14 samples, but, since the CO_2 is usually injected into the sandstone or carbonate reservoir, the shale and anhydrite samples are excluded. With these 11 samples, the mean and standard deviation of each parameter are estimated (**Table 6**). Under an assumption that all of the parameters follow the truncated normal distribution, the mean and standard deviation give the probability density function for each parameter. **Fig. 6** shows the normalized histogram and the estimated probability density function on each parameter. **Fig. 7** shows the cumulative probability distribution function with selected percentiles (P10, P30, P50, P70 and P90). The selected values are summarized in **Table 7**. **Fig. 8** shows the relative permeability curves to be used in the sensitivity study for each parameter. We have 17 relative permeability curves in total, and simulation will be run using each of them.

TABLE 6 - STATICTICS OF THE SAMPLES

Parameter	Mean	Standard deviation (Sample)	Variance (sample)
$S_{brine,ir}$	0.456	0.140	0.0197
Brine Exponent	2.04	0.716	0.513
CO_2 exponent	3.20	1.71	2.94
$k^0_{r,CO2}$	0.270	0.185	0.0340

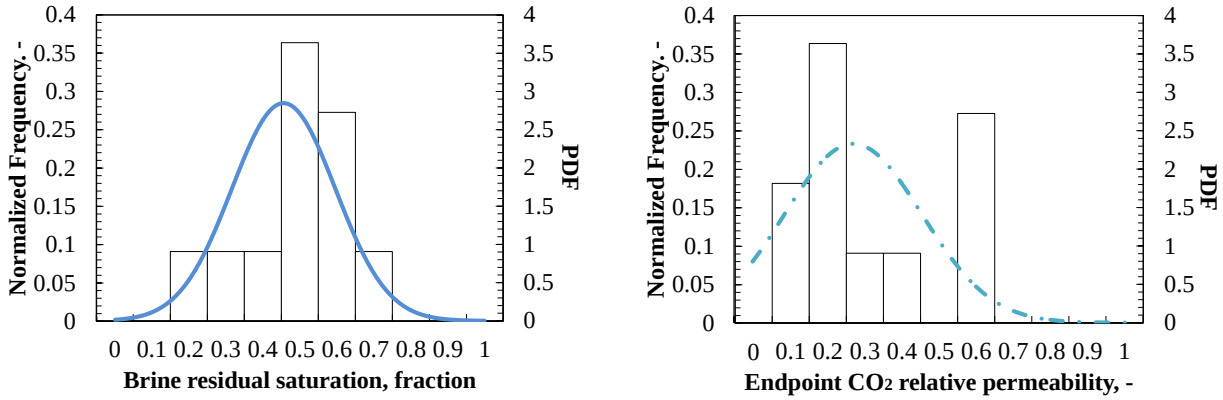

(a) Residual brine saturation (b) Endpoint CO_2 relative permeability

Fig. 6 – Normalized frequency and probability density function for the parameters in the relative permeability model

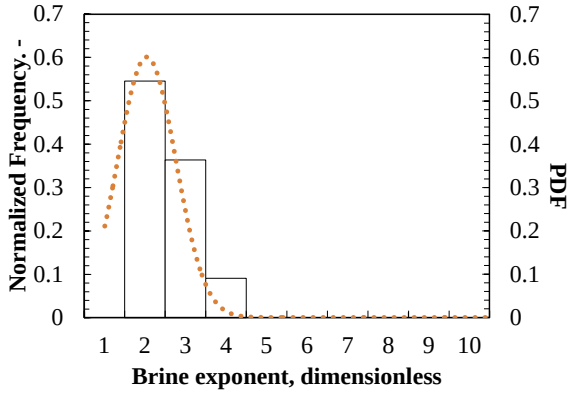

(c) Brine exponent

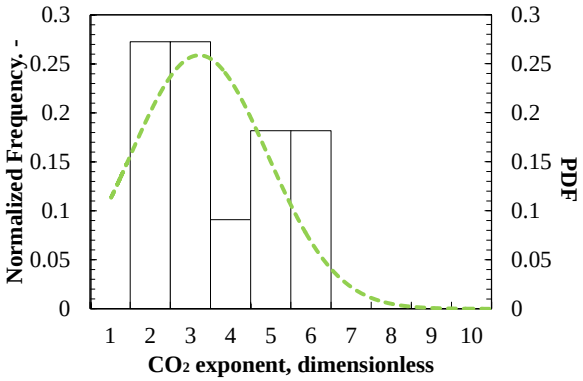

(d) CO_2 exponent

Fig. 6 – (*continued*) Normalized frequency and probability density function for the parameters in the relative permeability model

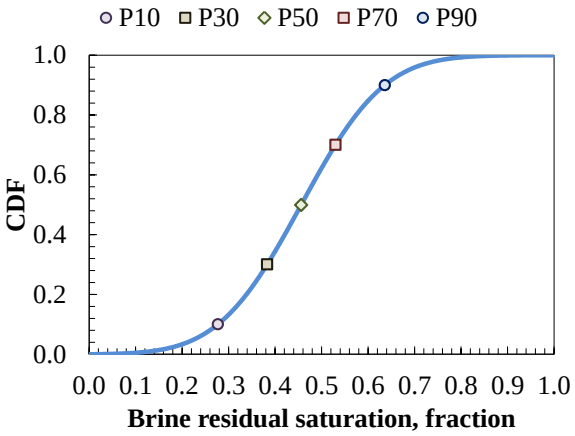

(a) Brine residual saturation

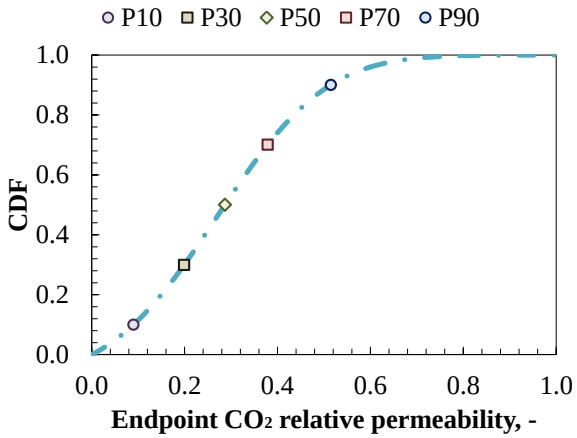

(b) Endpoint CO_2 relative permeability

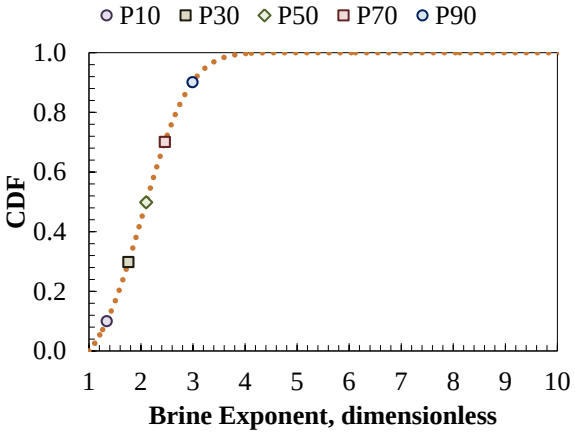

(c) Brine exponent

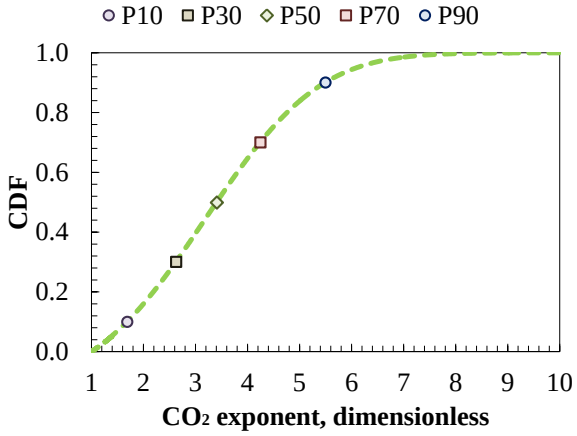

(d) CO_2 exponent

Fig. 7 – Cumulative distribution function with selected percentiles (P10/P30/P50/P70/P90)

TABLE 7 - VALUES AT THE SELECTED PERCENTILES					
	CDF Percentiles				
Parameter	P10	P30	P50	P70	P90
$S_{brine,ir}$	0.277	0.383	0.456	0.530	0.636
Brine exponent	1.34	1.76	2.10	2.46	2.99
CO_2 exponent	1.69	2.63	3.41	4.25	5.50
$k^0_{r,CO2}$	0.0900	0.199	0.287	0.379	0.515

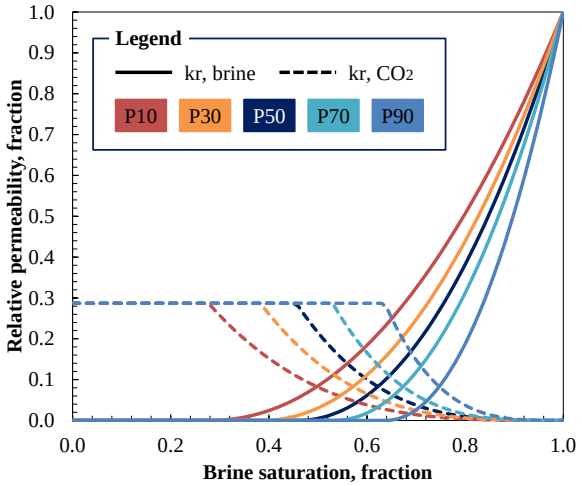

(a) Brine residual saturation

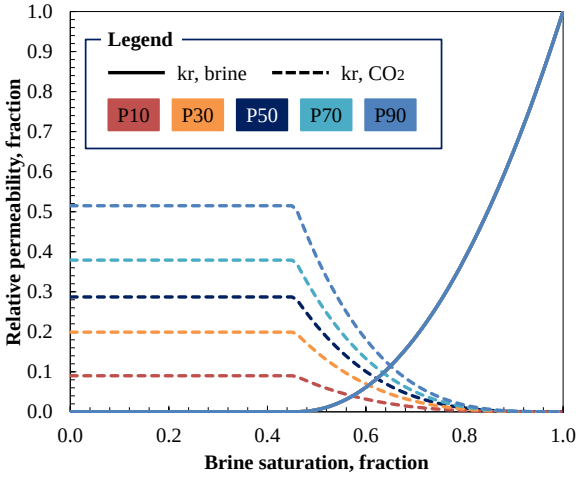

(b) Endpoint CO_2 relative permeability

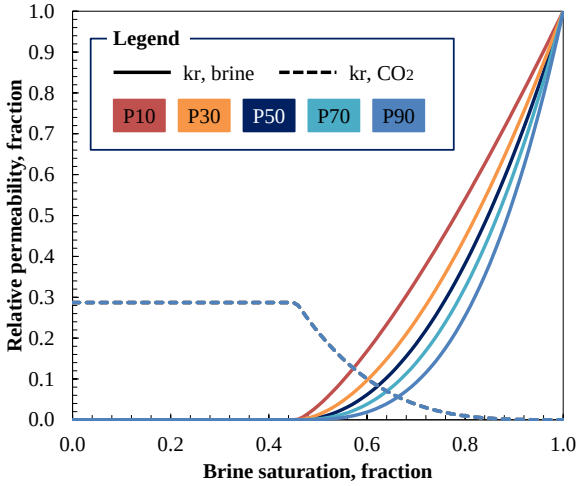

(c) Brine exponent

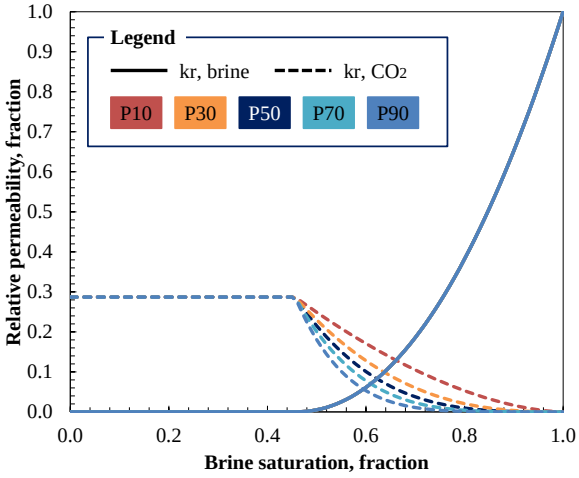

(d) CO_2 exponent

Fig. 8 – Relative permeability curves for the parameter sensitivity study

3.2 Sensitivity study results and discussion

Seventeen simulations are performed with the relative permeability curves shown in Fig. 8 and parameters summarized in Table 1 under constant pressure injection for 4 years. **Fig. 9** shows the total amount of injected CO_2 in 10^6 kg versus each parameter in the relative permeability model and the maximum CO_2 effective permeability. According to these plots, it is observed that the residual brine saturation and endpoint CO_2 relative permeability (maximum CO_2 effective permeability) has the positive relationship with the total injected CO_2 amount, and the brine exponent and CO_2 exponent show the negative relationship. **Fig. 10**, **Fig. 11**, **Fig. 12** and **Fig. 13** are the contour plots of the CO2 plume after 4 years injection for each case of the sensitivity study, which are the cases of residual brine saturation, brine exponent, CO_2 exponent and endpoint CO_2 relative permeability, respectively. For the negative relationship in the cases of brine and CO_2 exponent, the increase of the exponent value leads to the reduction of mobility or effective permeability of each phase for entire region except the highest and lowest relative permeability, and it requires more injection pressure to keep the same injectivity to base case. In Fig. 11, since the CO_2 relative permeability is not changed, the location and the shape of the saturation front seems not to be changed so much. However, the higher CO_2 saturation region is reduced as the brine exponent increase. In Fig. 12, it is clearly showed that, with the increase of the value of CO_2 exponent, the CO_2 plume size is reduced and the saturation front shows the steep saturation change in the case of higher value of CO_2 exponent. Oppositely, the increase of the endpoint CO_2 relative permeability augments the mobility or effective permeability of CO_2 especially at the saturation front, and then the injectivity increases. Fig. 13 shows the advancement of the saturation front with the increase of the endpoint CO_2 relative permeability at the end of 4 years injection. The case of residual brine saturation looks more complex than the other parameters. The increase of the residual brine saturation gives the increase of the CO_2 effective permeability but also the decrease of the brine effective permeability at a given saturation. The former contributes to faster movement of the CO_2, but the latter prevent the water movement. And the increase of the residual brine saturation gives the reduction of the pore space for CO_2 to flow, and this contributes the increase of the saturation front velocity. In addition, in this work, the capillary pressure curve is fixed and does not change with the change of parameters used in the sensitivity study. It means that the increase of the residual brine saturation cause the decrease of the capillary pressure effect at the endpoint CO_2 saturation to the base case relatively. As we can see in Fig. 10, when the residual brine saturation is small, the saturation front stays near the injection location and higher saturation distribution in the region. With increase of the residual brine saturation, the saturation front moves ahead and the CO_2 saturation in the region becomes smaller. This is a trade-off between the speed of saturation front (sweep-zone of CO_2) and the storage capacity in the region, and in this problem, the effect by the advancement of the saturation front is larger (it holds higher injectivity). The general conclusion on the residual brine saturation requires more studies.

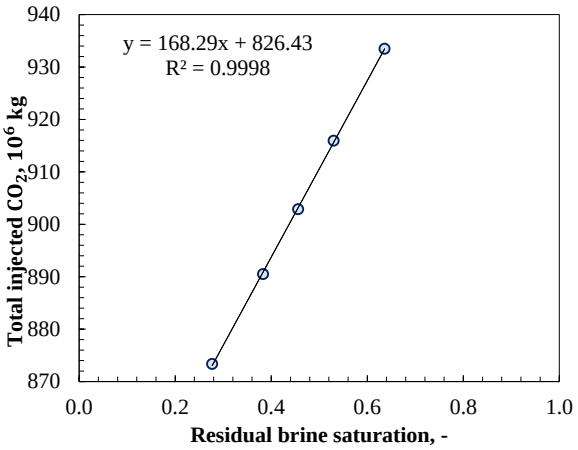

(a) Residual brine saturation

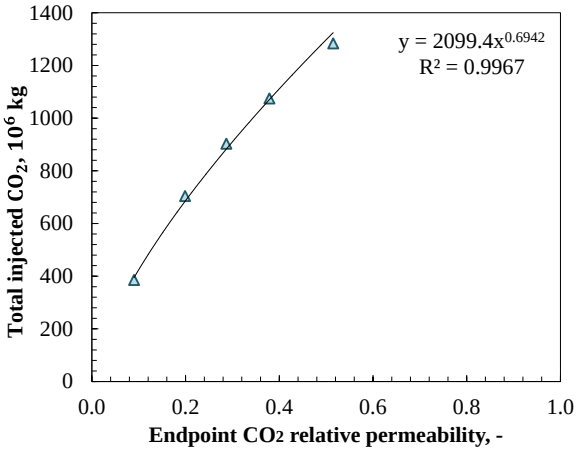

(b) Endpoint CO_2 relative permeability

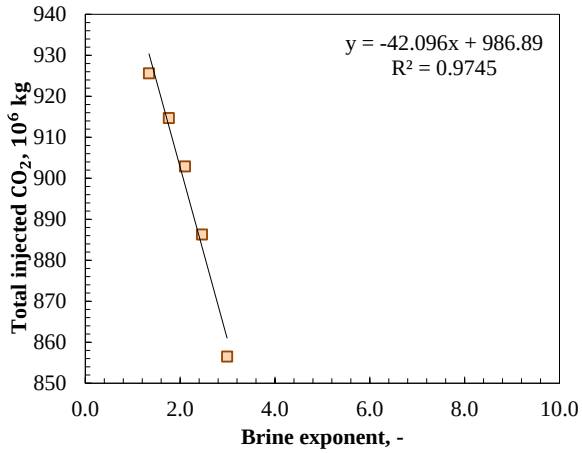

(c) Brine exponent

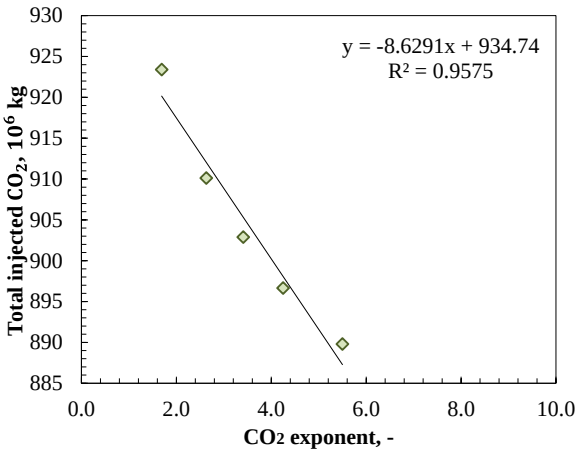

(d) CO_2 exponent

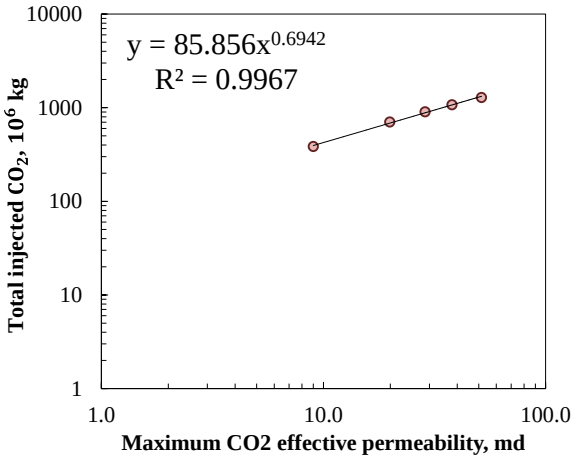

(e) Maximum CO_2 effective permeability

Fig. 9 – Injectivity to the parameters of the relative permeability model (sensitivity study)

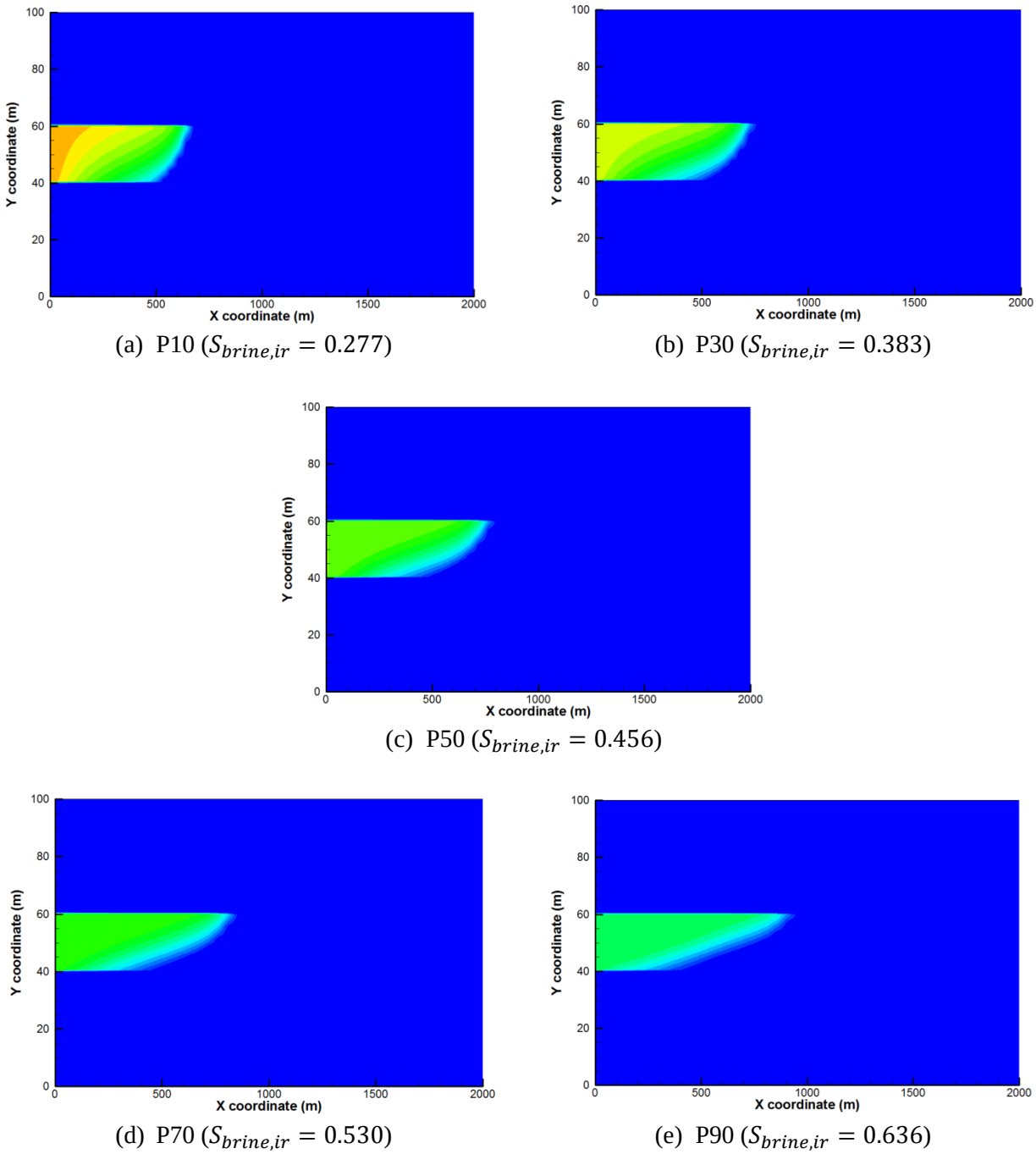

(a) P10 ($S_{brine,ir} = 0.277$)

(b) P30 ($S_{brine,ir} = 0.383$)

(c) P50 ($S_{brine,ir} = 0.456$)

(d) P70 ($S_{brine,ir} = 0.530$)

(e) P90 ($S_{brine,ir} = 0.636$)

Fig. 10 – CO2 plume after 4 years injection (sensitivity study on residual brine saturation)

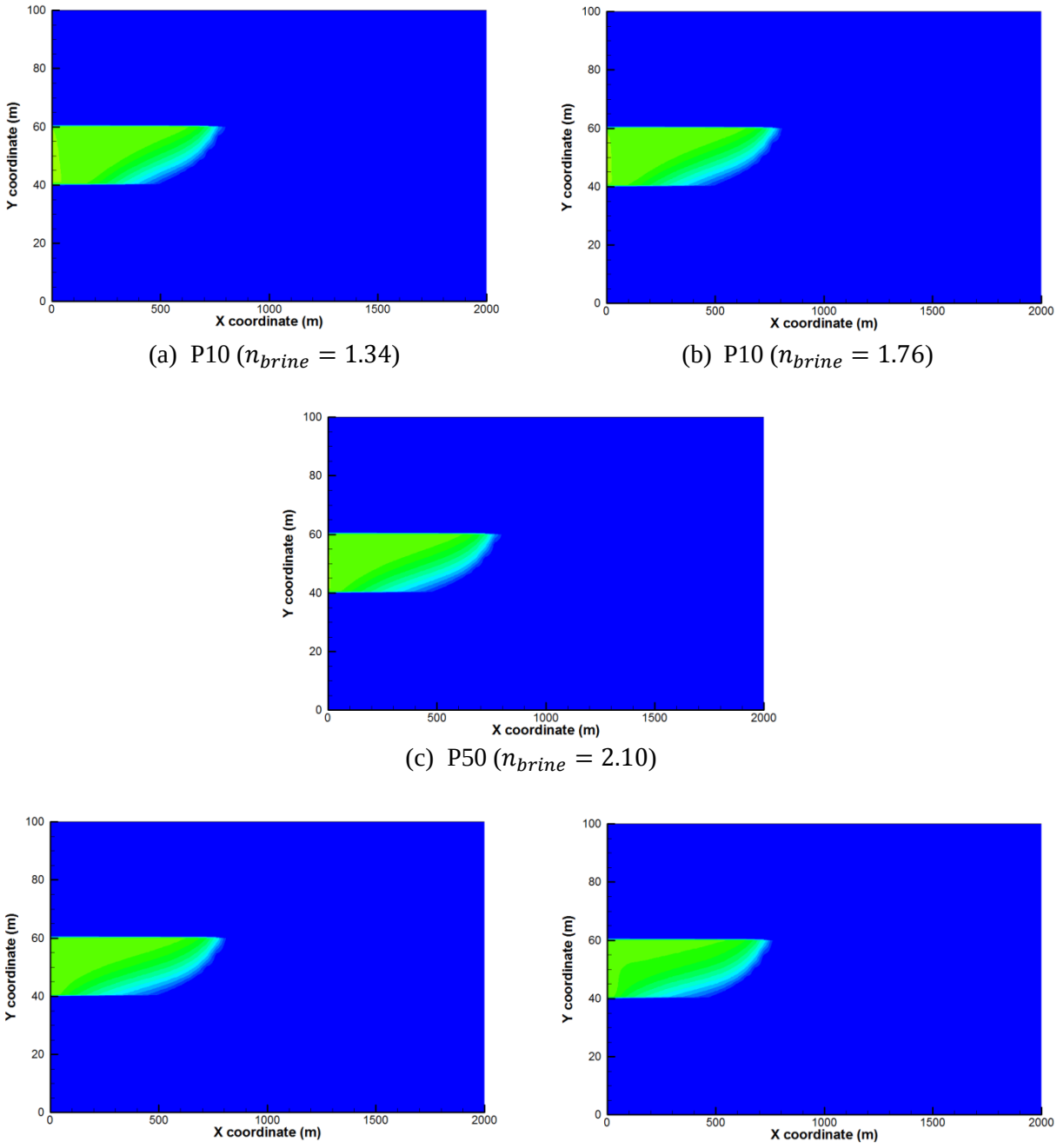

(a) P10 ($n_{brine} = 1.34$)

(b) P10 ($n_{brine} = 1.76$)

(c) P50 ($n_{brine} = 2.10$)

(d) P70 ($n_{brine} = 2.46$)

(e) P90 ($n_{brine} = 2.99$)

Fig. 11 – CO2 plume after 4 years injection (sensitivity study on brine exponent)

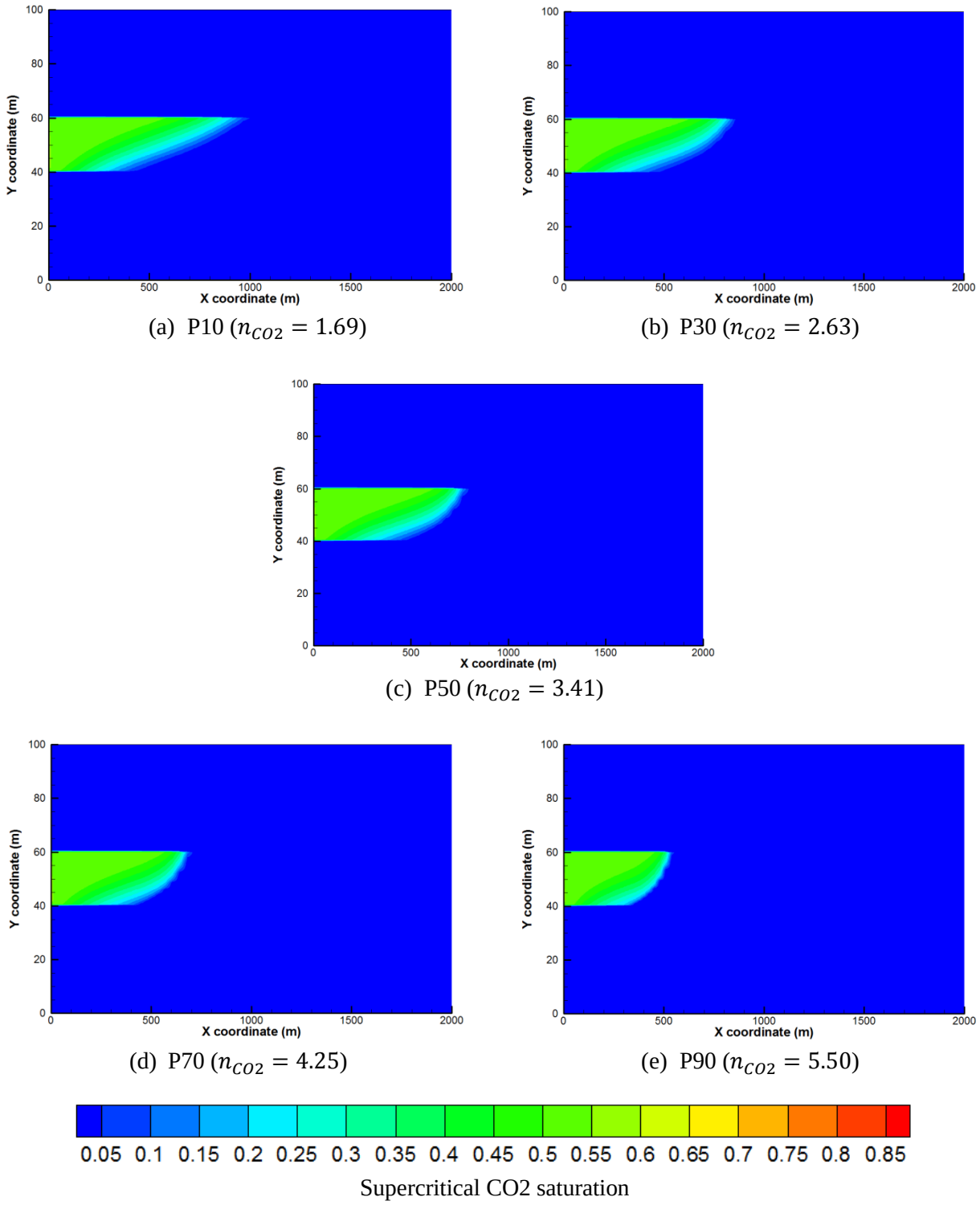

(a) P10 ($n_{CO2} = 1.69$)

(b) P30 ($n_{CO2} = 2.63$)

(c) P50 ($n_{CO2} = 3.41$)

(d) P70 ($n_{CO2} = 4.25$)

(e) P90 ($n_{CO2} = 5.50$)

Fig. 12 – CO2 plume after 4 years injection (sensitivity study on CO2 exponent)

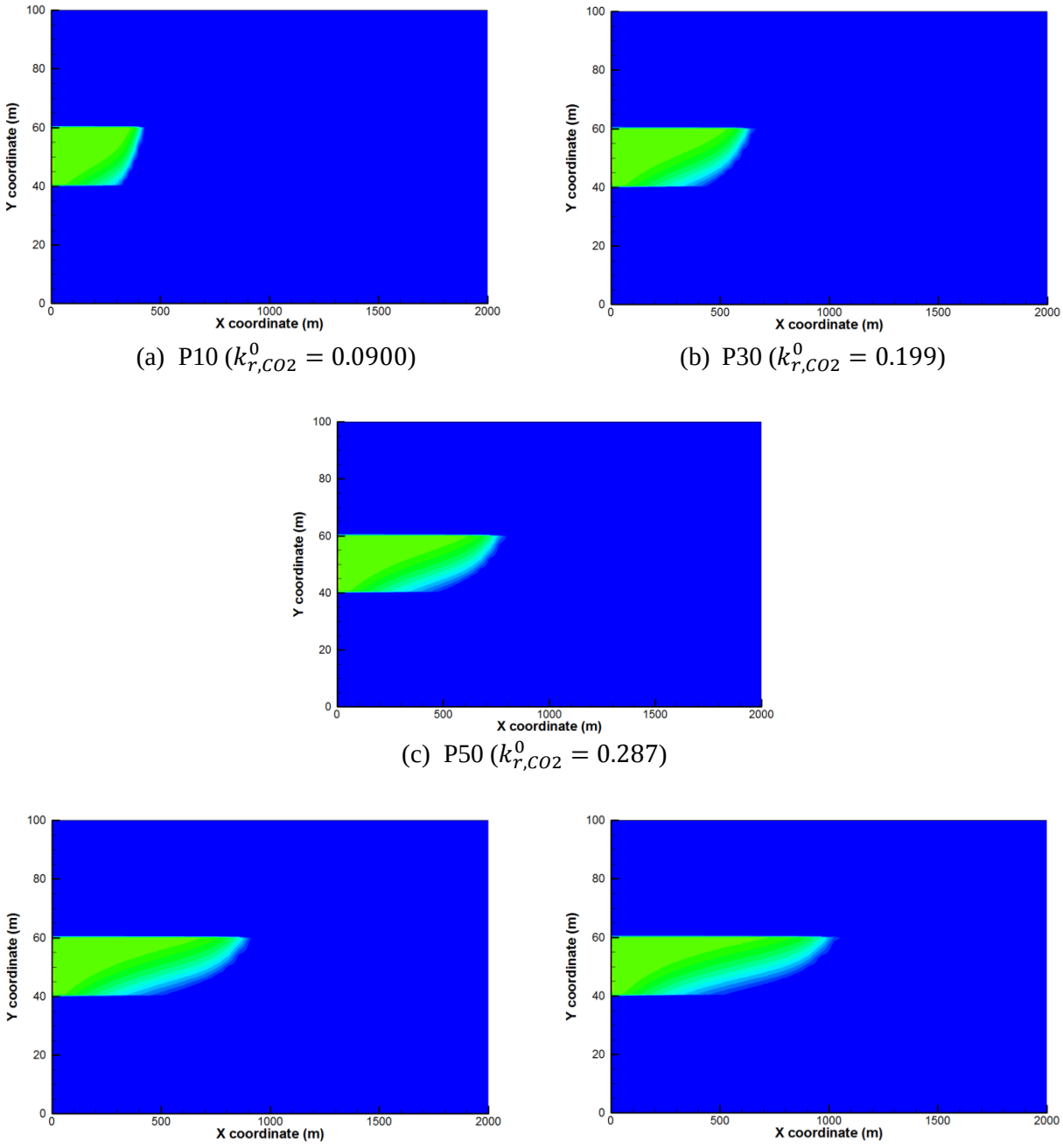

(a) P10 ($k^0_{r,CO2} = 0.0900$)

(b) P30 ($k^0_{r,CO2} = 0.199$)

(c) P50 ($k^0_{r,CO2} = 0.287$)

(d) P70 ($k^0_{r,CO2} = 0.379$)

(e) P90 ($k^0_{r,CO2} = 0.515$)

Fig. 13 – CO4 plume after 4 years injection (sensitivity study on residual brine saturation)

Each parameter behaves differently (positive or negative), but the magnitude of the sensitivity to the endpoint CO_2 relative permeability is much larger than the others. To see this clearly, **Fig. 14** shows the comparison plot of the amount of injected CO_2 with respect to the change of each parameter. Fig. 14 (a) is the comparison of the total injected CO_2 to the ratio of parameter change of each parameter, and it shows the difference of the magnitude clearly. In Fig. 14 (b), difference of the total injected CO_2 is expressed as the fraction to that of base case. Even if the residual brine saturation, brine exponent and CO_2 exponent are changed from P10 to P90, the change of injected CO_2 amount is within $\pm$10%, but, in the case of maximum CO_2 effective permeability, the change of CO_2 amount is nearly 60%. This confirms that the endpoint CO_2 relative permeability or the maximum CO_2 effective permeability has the dominant effects on the injectivity to the other parameters in the relative permeability model quantitatively.

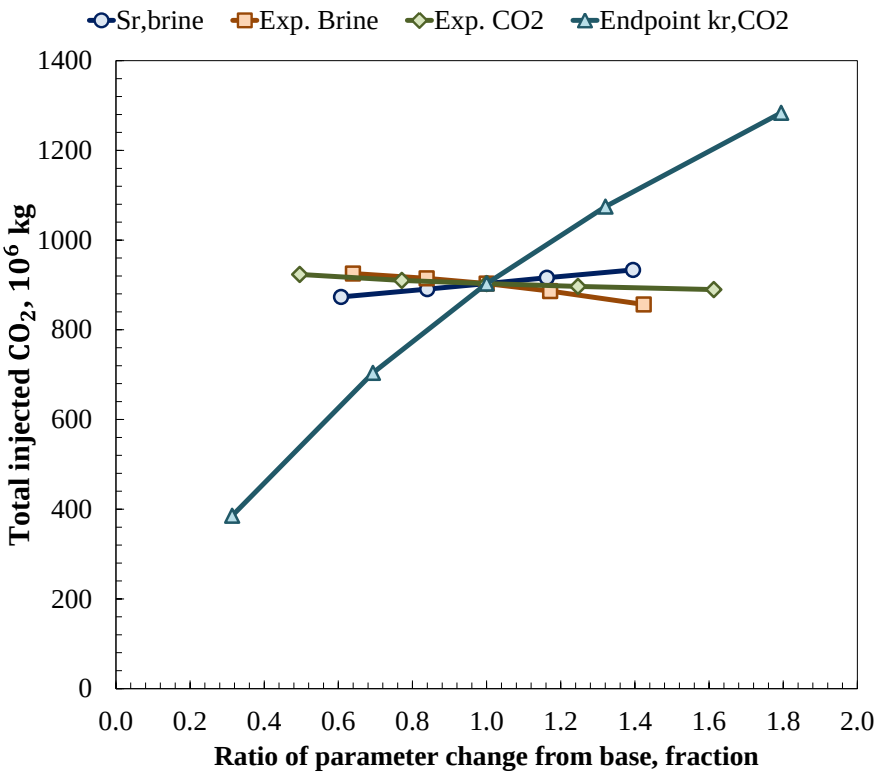

(a) Total injected CO_2 change to the ratio of each parameter change

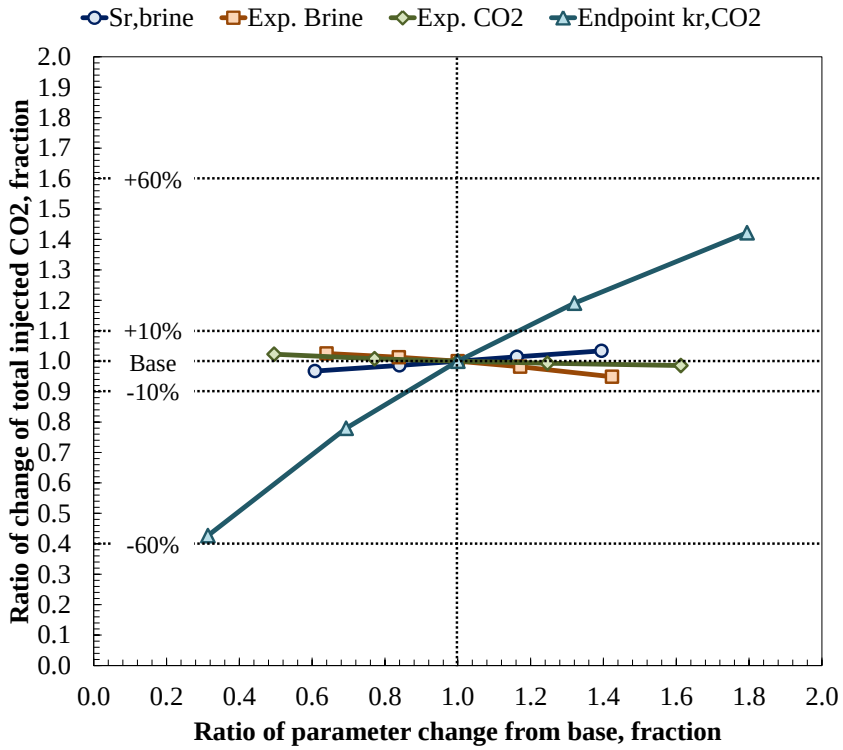

(b) Ratio of total injected CO_2 change to the ratio of each parameter change

Fig. 14 – Sensitivity analysis

3.3 Summary of sensitivity study

Through the parameter sensitivity study, it is confirmed that the endpoint CO_2 relative permeability or the maximum CO_2 effective permeability has the dominant role for the CO_2 injectivity comparing to the other parameters (i.e. brine exponent, CO_2 exponent and residual brine saturation). Though the relationship with the injectivity and the parameters is examined and the physical interpretation is performed to account for it, the magnitude of the injectivity change caused by all of the parameters except the endpoint CO_2 relative permeability is at most plus/minus 10% and it is quite small comparing to 50-60% by the endpoint CO_2 relative permeability.

Based on the sensitivity study, we quantify the sensitivity of the injectivity to the parameters in the relative permeability model. These results suggest it is sufficient to consider the uncertainty only by the end point CO2 relative permeability for the risk analysis performed in the reduced-order model such as CO2-PENS. This is consistent with the conclusion implied by the preliminary study in the previous section. Since this sensitivity study is based on the small amount of data given by Bennion and Bachu (2008), in the next section, we run the Monte Carlo simulation with sufficient realizations to calibrate the above conclusion/suggestion.

4 Monte Carlo Simulation for Calibration

4.1 Objectives and approach

Objectives of this section are 1) to quantify the uncertainty caused by variation of relative permeability curve against the target problem, 2) to calibrate the conclusion/suggestion given by the parameter sensitivity study with sufficient realizations, and 3) to investigate the possibility of the utilization of the curve subsampling method. In this Monte Carlo simulation, we employ the Latin Hypercube Sampling to efficiently reduce the number of realization because each simulation run by FEHM is computationally expensive. The underlying probability density function of each parameter in the extended Corey's model is summarized in the previous. We start to run simulations with the smallest amount of realization, and increase the number of realization with checking the convergence of the Monte Carlo method.

4.2 Sampling method

As the sampling method, the Latin Hypercube Sampling is adopted for the Monte Carlo simulation runs. The Latin Hypercube Sampling divides the cumulative distribution function into several intervals (corresponding to the number of realization) for each parameter, and each interval cell has the same probability (**Fig. 15** (a)). Then, from the corresponding parameter intervals, samples are randomly selected for each parameter. Fig. 15 (b) shows the two-dimensional representation as one possible LHS with 5 realizations. In this problem, as it was mentioned above, we use the probability density function specified in the previous section, and generate the curves for the cases of 25 realizations, 50 realizations, 100 realizations and 1000 realizations. The generated realizations are summarized in the appendix (**Table A.1**, **A.2** and **A.3** for 25, 50 and 100 realizations, respectively). **Fig. 16** and **Fig. 17** show the realizations of brine relative permeability curves and CO_2 relative permeability curves, respectively. As we can see, the realizations of the brine relative permeability curve create the clusters, and they look similar to the realizations of the retention curves shown by Stauffer and Lu (2011). On the other hand, the CO_2 relative permeability curves seem to be scattered especially for the case of 25 realizations. The curves create the cluster in the case of 50 realizations, and this is consistent with the plots by 100 realizations and 1000 realizations. So, 50 or 100 realizations are assumed to be required to obtain the converged results.

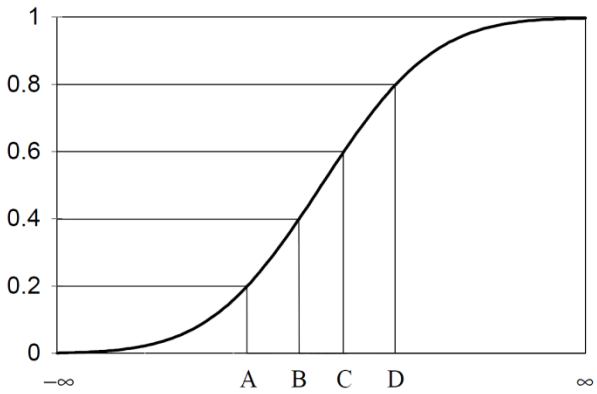

(a) Intervals by LHS for normal distribution with 5 realizations

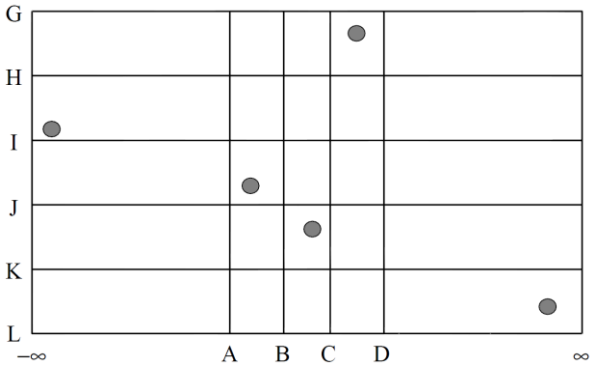

(b) A two-dimensional representation of one possible LHS with 5 realizations

Fig. 15 – Schematics of the example case of Latin Hypercube Sampling (taken after Wyss et al., 1998)

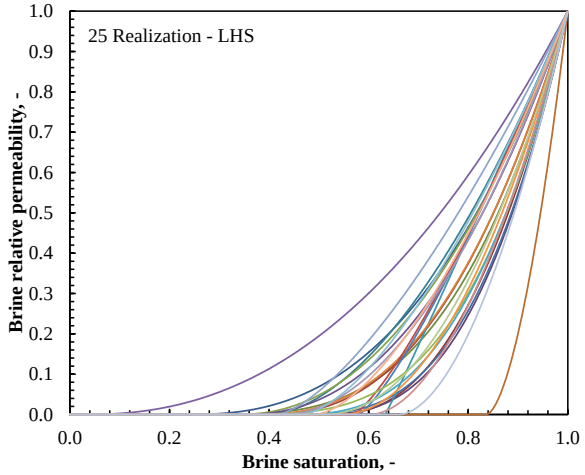

(a) 25 realization

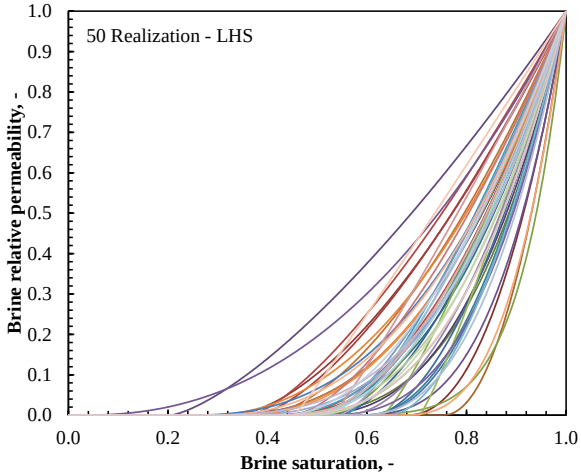

(b) 50 realization

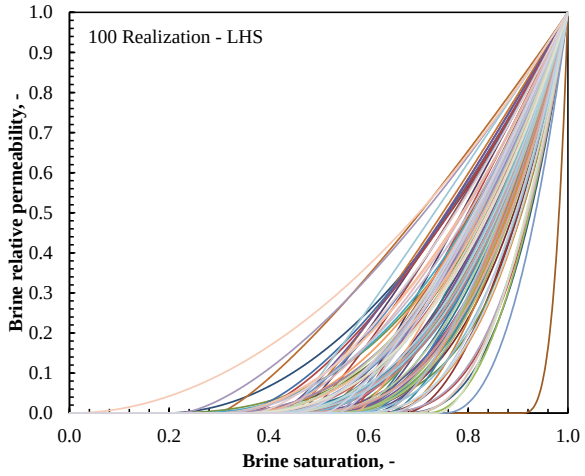

(c) 100 realization

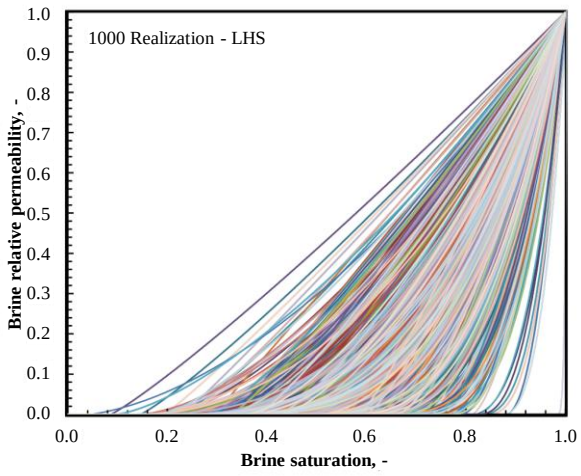

(d) 1000 realization

Fig. 16 – Realizations of brine relative permeability curve (25/50/100/1000 realizations)

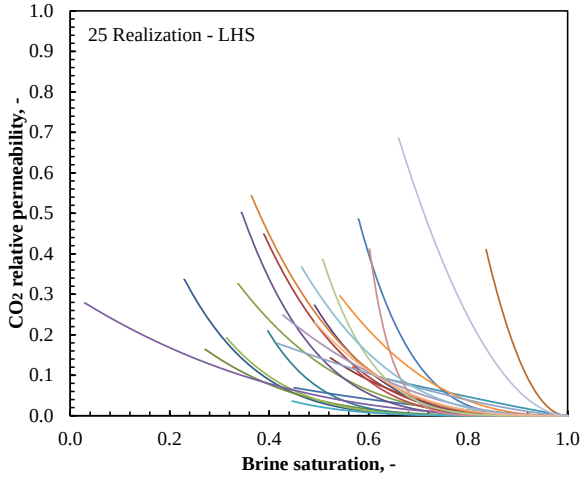

(a) 25 realization

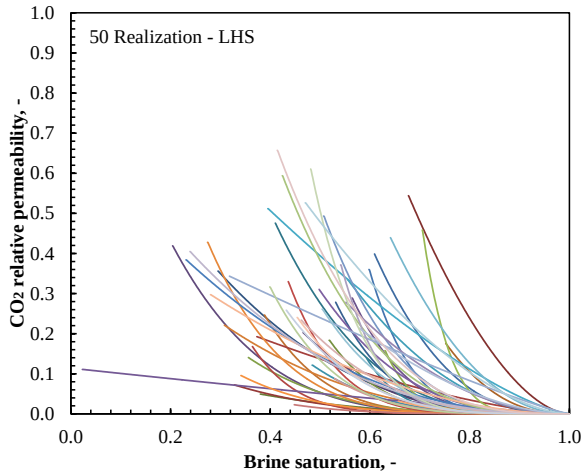

(b) 50 realization

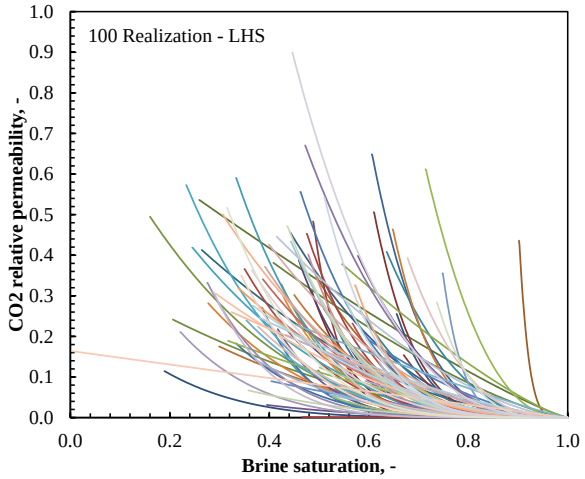

(c) 100 realization

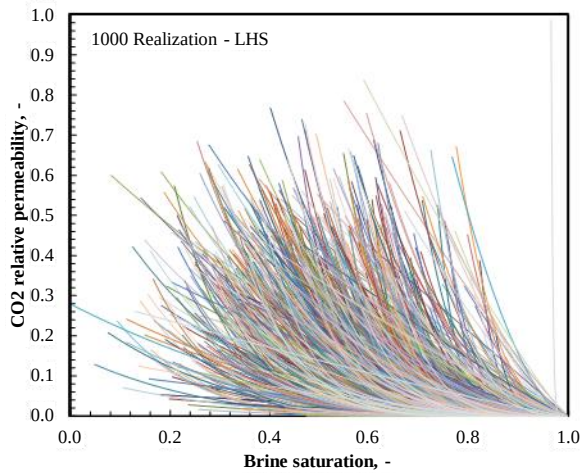

(d) 1000 realization

Fig. 17 – Realizations of CO_2 relative permeability curve (25/50/100/1000 realizations)

4.3 Results

Uncertainty quantification

At first, in order to check the convergence of the Monte Carlo simulation, the plots of cumulative injected CO_2 are compared among the different number of realizations. **Fig. 18** shows the results of the total injected CO_2 with respect to time for the different numbers of realization. The gray lines in these plots are the results given by each realization. The red line, dark blue line, green line and the clear blue line show the mean, median, mean – σ (standard deviation), and mean + σ, respectively. **Table 8** is the summary of the statistical values given by the different set of realizations on the total injection volume at 4 year. The mean and standard deviation values are changed by around 4×10^6 kg and 7×10^6 kg between the 25 realization case and 50 realization cases. On the other hand, the change between 50 and 100 cases is reduced within 1×10^6 kg.

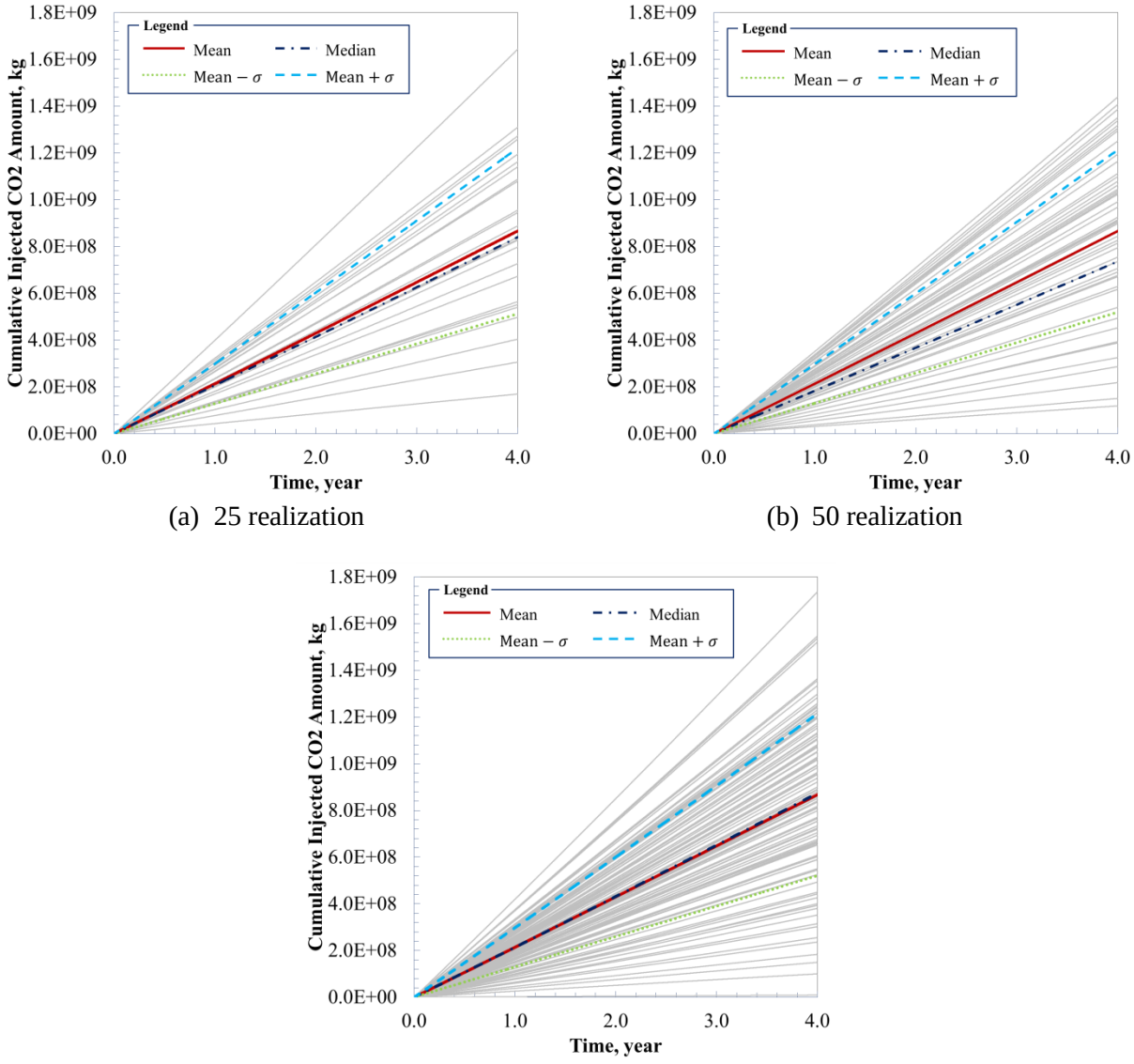

(a) 25 realization

(b) 50 realization

(c) 100 realization

Fig. 18 – Total injected CO_2 vs. time (25/50/100 realizations)

TABLE 8 - STATISTICAL VALUES FOR TOTAL INJECTED CO_2 AT 4 YEAR			
	Number of realizations		
Parameter	25	50	100
Mean, 10^6 kg	861.451	865.916	865.074
Standard deviation, 10^6 kg	354.074	346.801	347.012
Median, 10^6 kg	839.842	901.348	873.587

Fig. 19, **Fig. 20** and **Fig. 21** show statistical distributions for the cases of 25, 50 and 100 realizations, respectively. According to the histograms, the probability distribution of the total injected CO_2 is assumed to follow the normal distribution and the cumulative distribution function by the data and the theoretical distribution given by the mean and standard deviation summarized in Table 7 are also shown in these figures. Comparing these cumulative distribution functions, the 50 realization case seems to be sufficient with consideration of the variation of the statistical parameters (mean and standard deviation). We focus on the results given by the 100 realizations in the rest of the report.

In addition to the total injected CO_2, the injection rate after 4 years injection is examined and the statistical distribution is shown in **Fig. 22**. The injection rate is also assumed to follow the normal distribution on the histogram, and the cumulative distribution function is shown. In **Table 9**, the detail statistical parameter values are summarized for both the total injection volume and the injection rate, and the box plot is shown in **Fig. 23**. Here, the standard deviation of the total injected CO_2 is 347.012 10^6 kg, and the ±40% of the mean value is within 1-standard deviation range (about 70%). This is corresponding to the injection rate, because the standard deviation of the injection rate is 2.849 kg/s and this is the 40% of the mean value (6.980 kg/s) of the injection rate at the end of 4 years CO_2 injection. According to these results, it can be stated that the total injected CO_2 and the injection rate or injectivity vary within ±40% at the possibility of about 70% even if only the relative permeability curve changes.

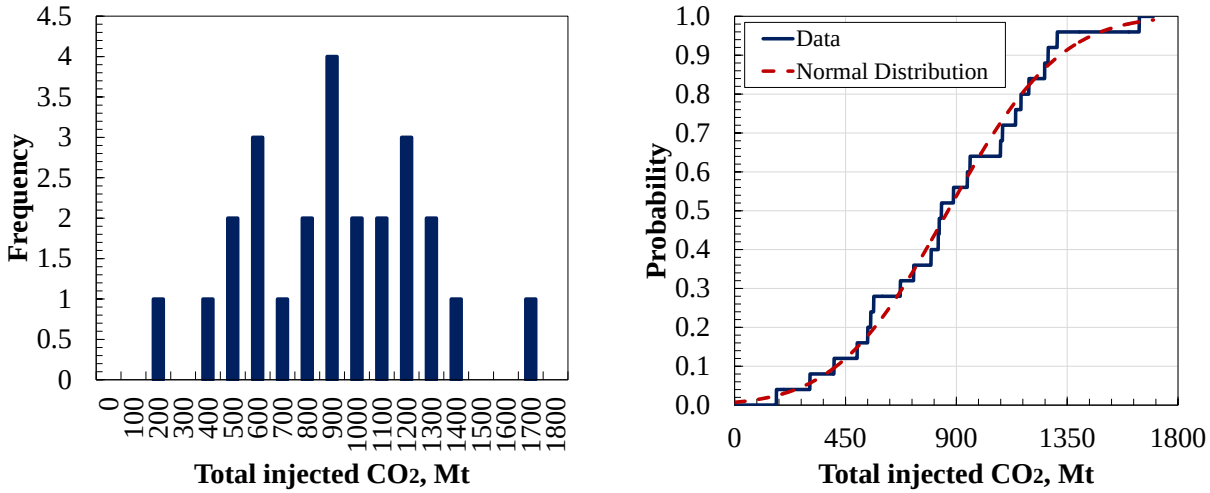

(a) Histogram (b) Cumulative distribution function

Fig. 19 – Statistical distribution of total injected CO_2 (25 realizations)

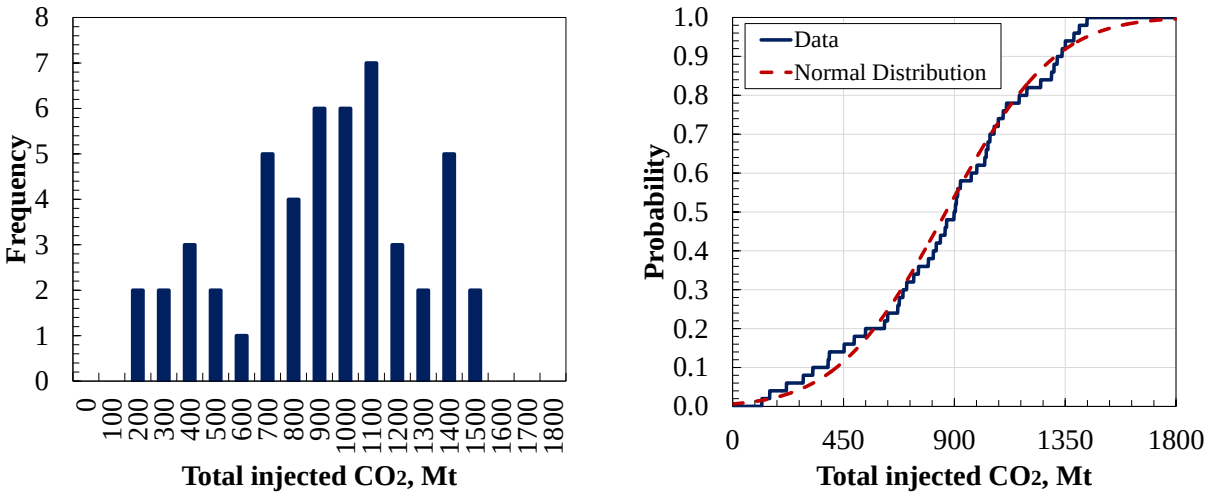

(a) Histogram (b) Cumulative distribution function

Fig. 20 – Statistical distribution of total injected CO_2 (50 realizations)

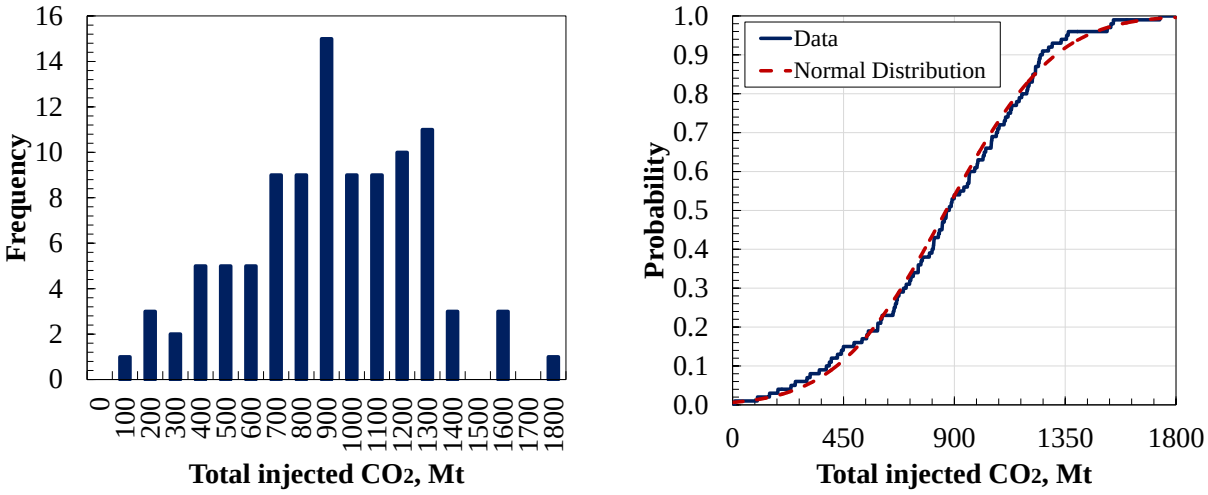

(a) Histogram (b) Cumulative distribution function

Fig. 21 – Statistical distribution of total injected CO_2 (100 realizations)

TABLE 9 – VALUES FOR BOX PLOT (TOTAL INJECTED CO_2 AND INJECTION RATE)

Parameter	Total injected CO_2, 10^6 kg	Injection rate (at 4 years), kg/s
Minimum	8.897	0.06838
25% Percentile	659.4	5.248
Median	873.6	7.105
Mean	867.0	6.980
75% Percentile	1121	9.013
Maximum	1735	14.24

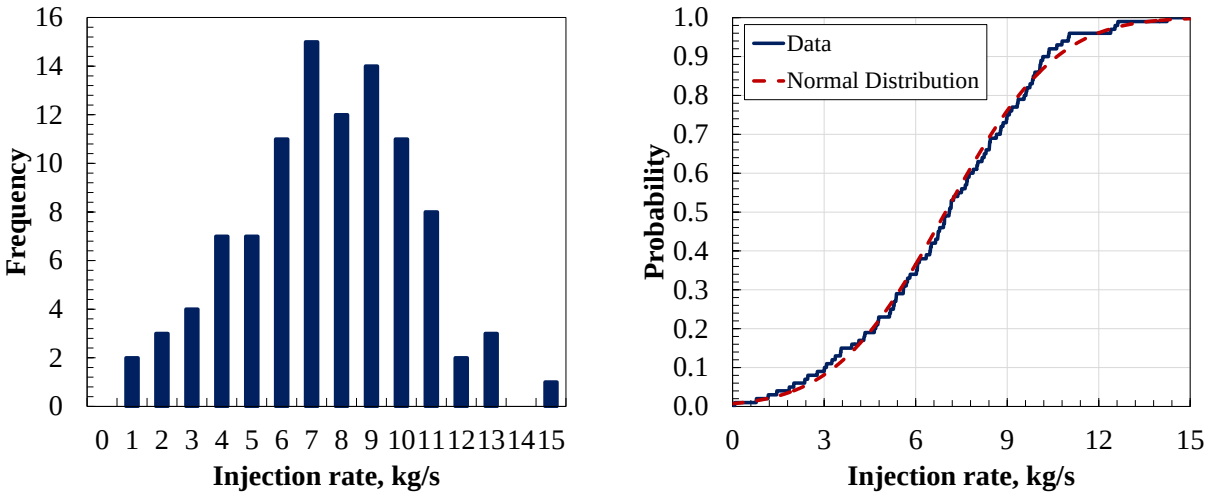

(a) Histogram (b) Cumulative distribution function

Fig. 22 – Statistical distribution of injection rate at 4 years injection (100 realizations)

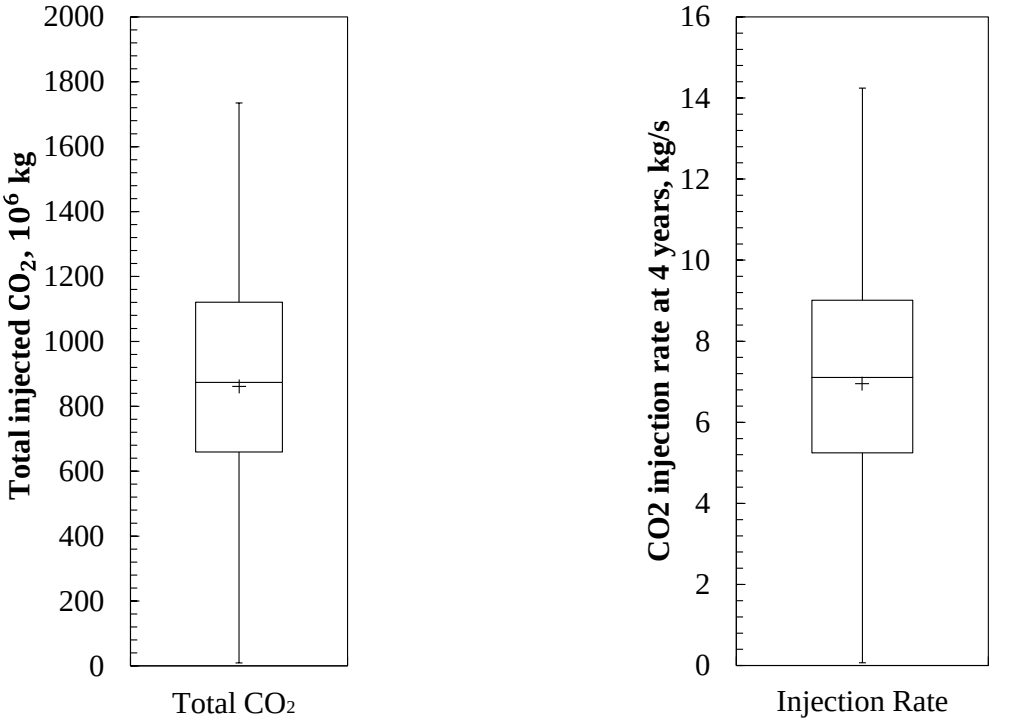

(a) Total injected CO_2 (b) Injection rate at the end of 4 year injection

Fig. 23 – Box plot for total injected CO_2 and the injection rate at the end of 4 year injection

Calibration of the conclusion/suggestion given by the parameter sensitivity study

Fig. 24 shows the results of the total injected CO_2 to the parameters in the relative permeability model given by 100 realizations. As we can see, the residual brine saturation, brine exponent and CO_2 exponent does not have the strong relationship to the total injected amount, but the endpoint CO_2 relative permeability does. Through the parameter sensitivity study, we concluded that the endpoint CO_2 relative permeability has the dominant effect on the total injected volume though the other parameter has the relationship to the total injection amount and the magnitude is quite small to that of endpoint CO_2 relative permeability. Therefore, the results given here is consistent with the sensitivity study (the effect by the other parameter is masked by the effect of endpoint CO_2 relative permeability). In **Fig. 25**, the plots of the total injection volume to the endpoint CO_2 relative permeability and the maximum effective CO_2 permeability are shown in the log-log axis. The regression lines are also shown in the plot with the equation and the R^2 value. The trend lines which have best performance are expressed in the form of power relationship, and the R^2 values are more than 0.98 (correlation coefficient is near 0.99) and these are acceptable as the regression line. In addition to the total injected amount of CO_2, the injection rate at the end of 4 year injection to the parameters of the relative permeability model is also shown in **Fig. 26**. We can see almost same trend with the results of total injected CO_2 (Fig. 24), and, then, the injection rate to the endpoint CO_2 relative permeability and the maximum CO_2 effective permeability is same also (**Fig. 27**). At the end of years injection, the injection rate is already stabilized (**Fig. 28**). Since the stabilized injection rate determine the total injected CO_2 amount in long term injection, it is reasonable that these results look similar.

These results calibrate the conclusion by the sensitivity study that the endpoint CO_2 relative permeability or maximum CO_2 effective permeability has the dominant role for the determination of the total injected CO_2 amount. This conclusion highlights the importance of the work done by Levine (2011) to measure more accurate endpoint relative permeability by core flooding experiment.

It is helpful to understand what causes the deviation from the regression line. For example, some points in the Fig. 25 and Fig. 26 shows the deviation from the regression line. This also can be seen in the case of 50 realizations. Especially, the points of the lowest and the largest endpoint CO_2 relative permeability show the largest deviation from the regression line as shown in Fig. 25 and Fig. 26. The interpretation of the reason of the deviation is to be discussed in the discussion section of this report.

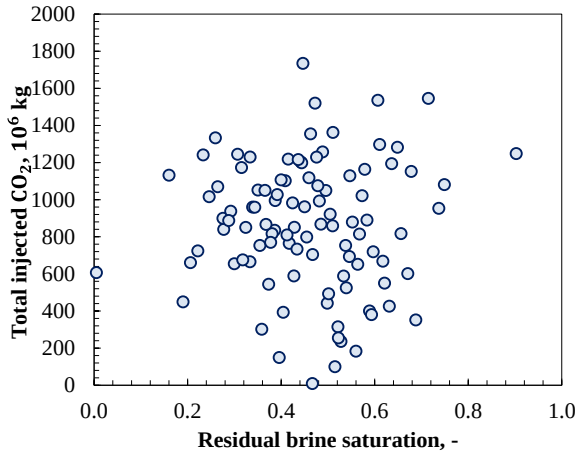

(a) Residual brine saturation

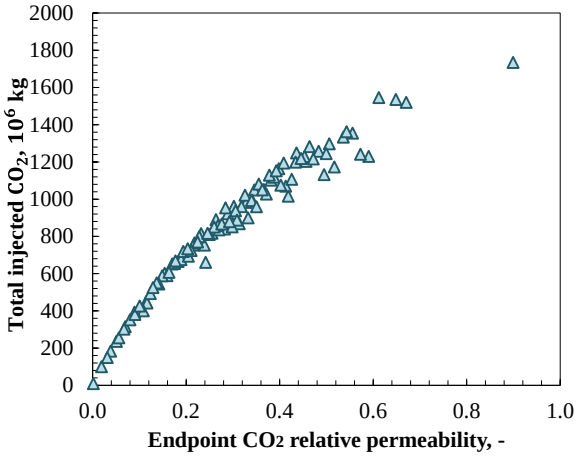

(b) Endpoint CO_2 relative permeability

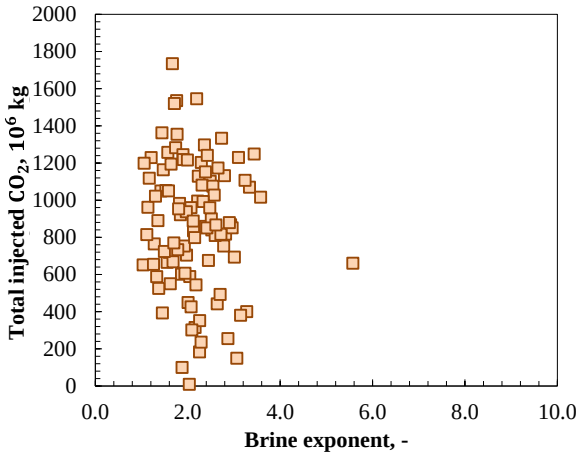

(c) Brine exponent

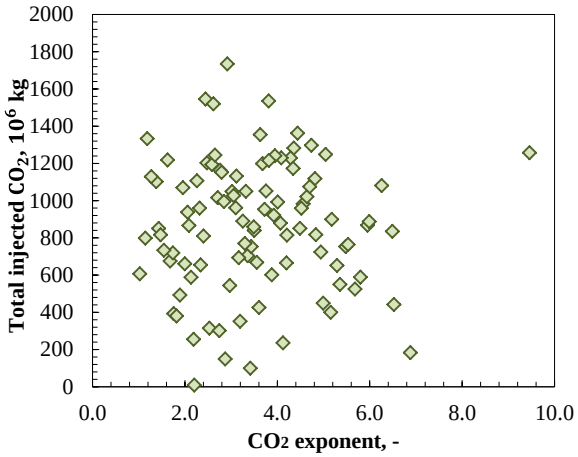

(d) CO_2 exponent

Fig. 24 – Total injected CO_2 to the parameters of the relative permeability model (100 realizations)

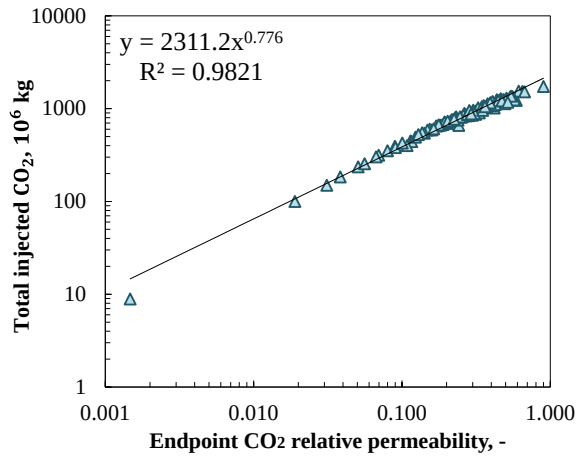

(a) Endpoint CO_2 relative permeability

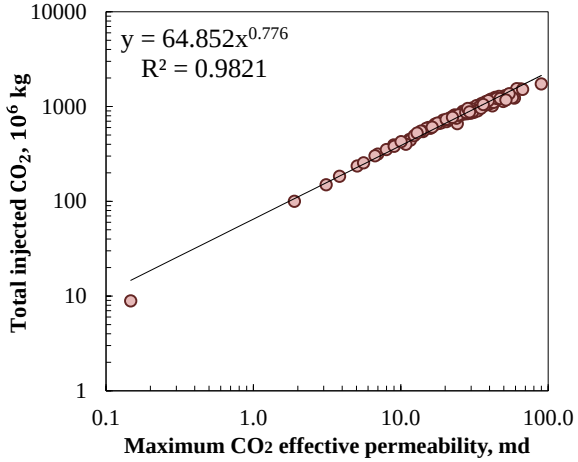

(b) Maximum CO_2 effective permeability

Fig. 25 – Total injected CO_2 to the endpoint relative permeability and the maximum CO_2 effective permeability (100 realizations)

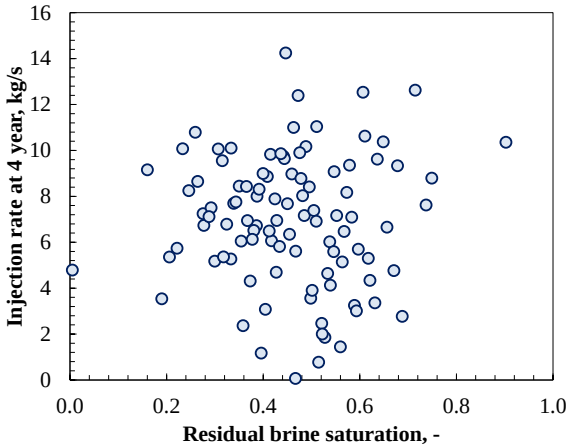

(a) Residual brine saturation

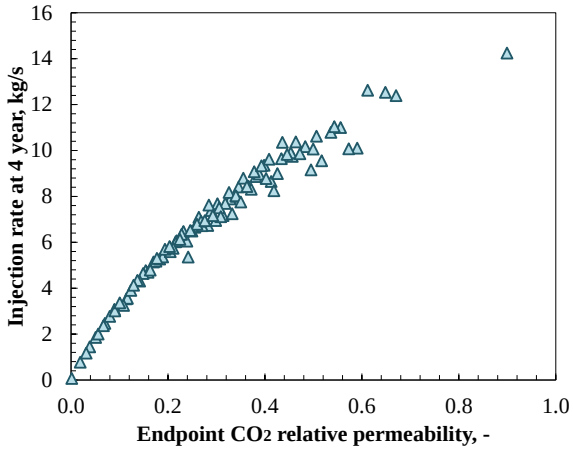

(b) Endpoint CO_2 relative permeability

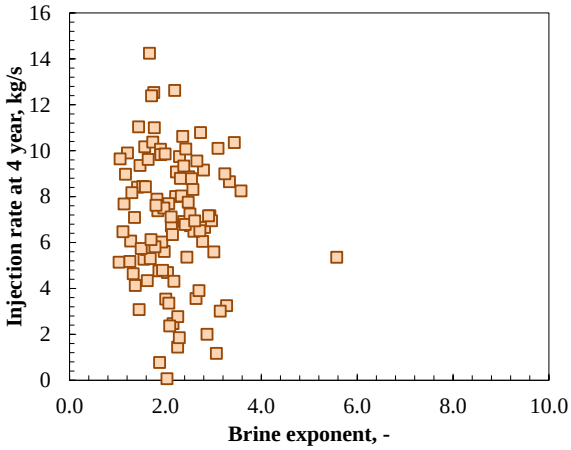

(c) Brine exponent

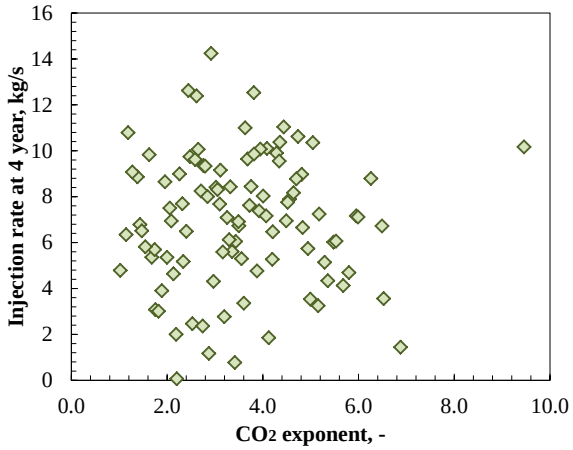

(d) CO_2 exponent

Fig. 26 – Injection rate at the end of 4 years injection to the parameters of the relative permeability model (100 realizations)

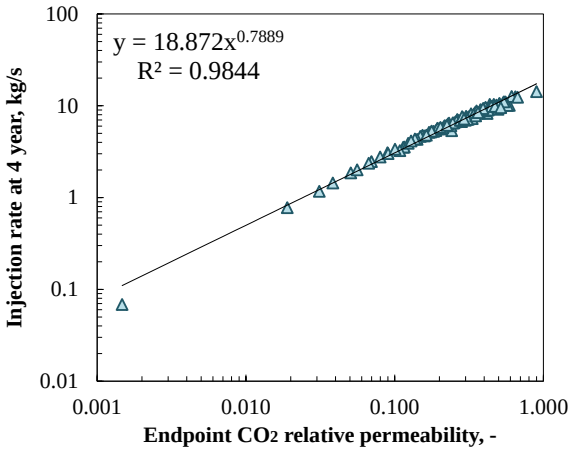

(a) Endpoint CO_2 relative permeability

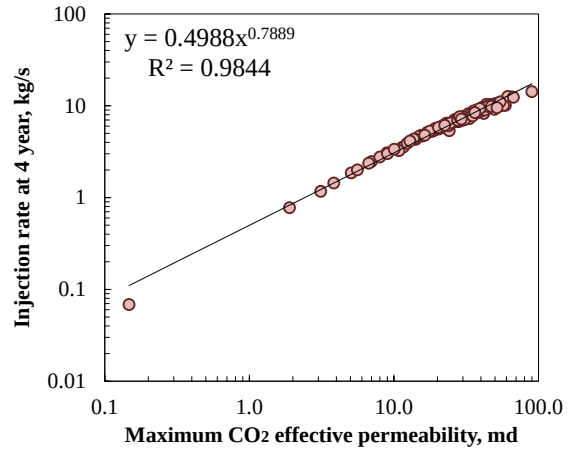

(b) Maximum CO_2 effective permeability

Fig. 27 – Injection rate at the end of 4 years injection to the endpoint relative permeability and the maximum CO_2 effective permeability (100 realizations)

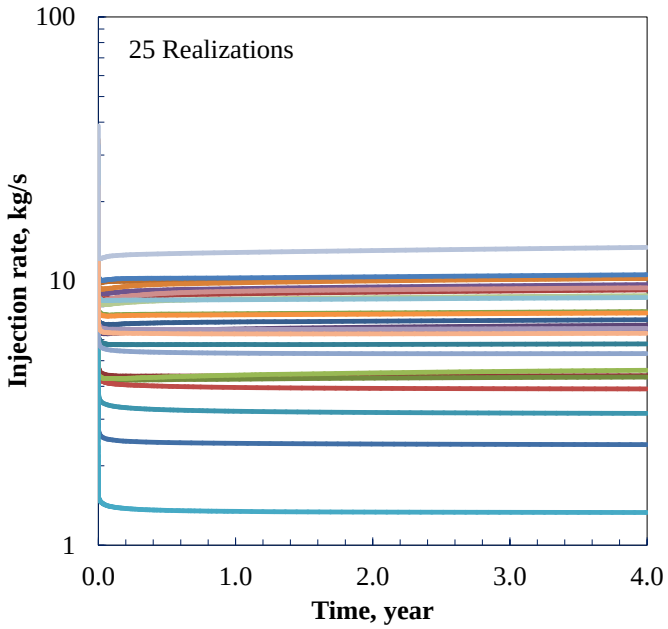

Fig. 28 – Injection rate history (25 realizations)

Investigation of the possibility of utilizing the curve subsampling method

As shown in Fig. 16 and Fig. 17, the brine relative permeability curves create clusters and it looks similar with the curves given by the retention curve (Stauffer and Lu, 2011). But, the CO_2 relative permeability curves look different from them. According to Stauffer and Lu (2011), their retention curve subsampling method was performed at the selected point of saturation. They concluded that the saturation value where the retention curves were sorted did not have a significant effect on the model results. However, in the case of the relative permeability, we need to consider how to perform the subsampling, because the liquid relative permeability curve does not exists at the saturation less than the residual brine saturation. In this case, for the liquid relative permeability curve, we can use the specified liquid relative permeability such as $k_{rl} = 0.5$, because all of the curves pass this point. On the other hand, the case of the CO_2 relative permeability is more complicated, because the range of the relative permeability depends on the endpoint CO_2 relative permeability also.

As we discussed in the calibration of the suggestion given by sensitivity study, the total injected amount of CO_2 and the injection rate at the end of 4 years injection have strong relationship to the endpoint CO_2 relative permeability, which masked the effects by the other parameters. Therefore, in this report, it is recommended to use only the endpoint CO_2 relative permeability as the variable for the subsampling or reduced-ordered model to quantify the uncertainty or the representative results for the simulation. The effects by the other parameters are also discussed in the discussion part.

4.4 Discussion

The results given by the parameter sensitivity study and the Monte Carlo simulation study show the solid positive relationship between the total injected CO_2 amount and the endpoint CO_2 relative permeability, which has the dominant role comparing to the other parameters: residual brine saturation, brine exponent and CO_2 exponent in the extended Corey's model. The Monte Carlo simulation provided the regression line for the total injected CO_2 amount with respect to the endpoint CO_2 relative permeability, and the power correlation has the excellent correlation coefficient under the homogeneous reservoir permeability distribution.

In this section, we discuss the reason for the deviation of the simulation results from the regression line. The regression line shown in the Monte Carlo simulation is explained by only one parameter (endpoint CO_2 relative permeability) for the sake of simplicity, but it provides excellent results as mentioned. Using the regression line, the possible error range of the simulation, the possible reasons for the error and their physical interpretations are discussed.

In **Fig. 29**, the plots of the total injected CO_2 amount to the endpoint relative permeability with the regression line. And, in the plot, several error-ranges (10%, 20% and 30%) from the regression line are also shown. As we can see in the Fig. 29 (a), the simulation results are mainly placed within around ±20% range. Fig. 29 (b) shows the same plot in the log-log scale except the data point with the minimum endpoint CO_2 relative permeability to confirm the simulation results are placed within the range clearly. **Fig. 30** shows the relative permeability curves out of 100 realizations which give more than ±10% error. These 15 CO_2 relative permeability curves show the error more than ±10% occurs in wide range of endpoint CO_2 relative permeability. Maximum error from the regression line occurs when the minimum endpoint CO_2 relative permeability is used, and the error is around 40% (the error magnitude is 6×10^6 kg). The endpoint relative permeability is, however, extremely small, and it provided the different trend curve comparing to the others (**Fig. 31**).

Fig. 32 shows the relative error of the simulation results from the regression line (except the maximum error data). As we can see, it is difficult to conclude the causes for the error by this plot, because, though the endpoint CO_2 relative permeability shows the weak negative relationship (correlation coefficient is 0.6859) shown in **Fig. 33**, the others do not show such relationship. The error seems to be caused by the combination of the parameters.

In this work, some extreme values were sampled. As we mentioned in the parameter sensitivity study, the endpoint CO_2 relative permeability has the dominant effect on the total injected CO_2 amount, but also the brine exponent is relatively sensitive to the other parameters (the magnitude of the slope is larger). Therefore, the largest value of the brine exponent caused the more than 10% deviation from the regression line (the effect of the brine exponent is large in the case). These extreme values are sampled by the Latin Hypercube Sampling used in this work, which divide the range of parameter into the number of realizations and sample one value from each segment randomly. This random sampling from each segment follows the uniform distribution in the region, and this cause the sampling of the extreme value. When the sampling is performed based on the true probability distribution function (in this case the tail of the normal distribution), these extreme values are avoided to be sampled.

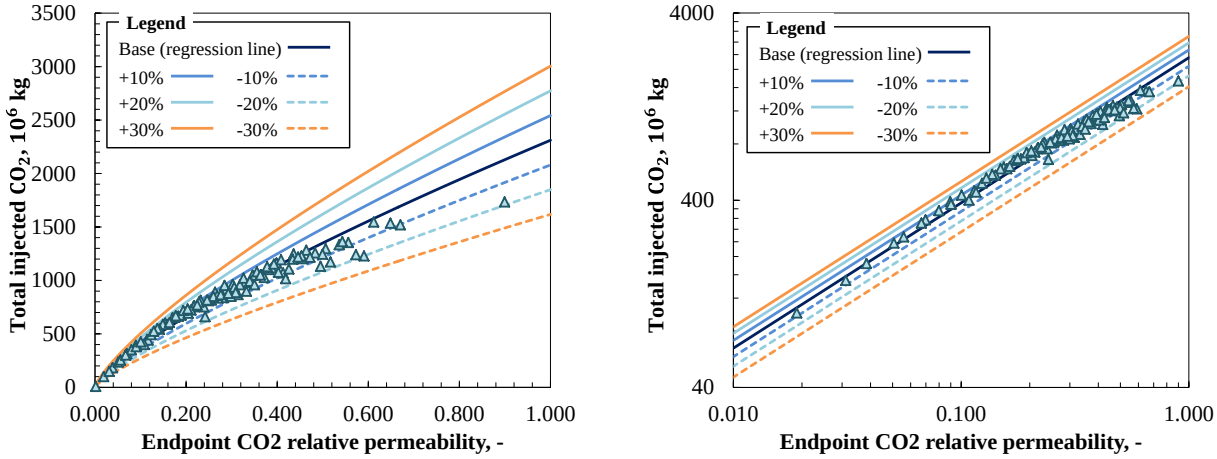

(a) Cartesian plot (b) Log-log scale plot

Fig. 29 – Total injected CO_2 amount with the error range from the regression line

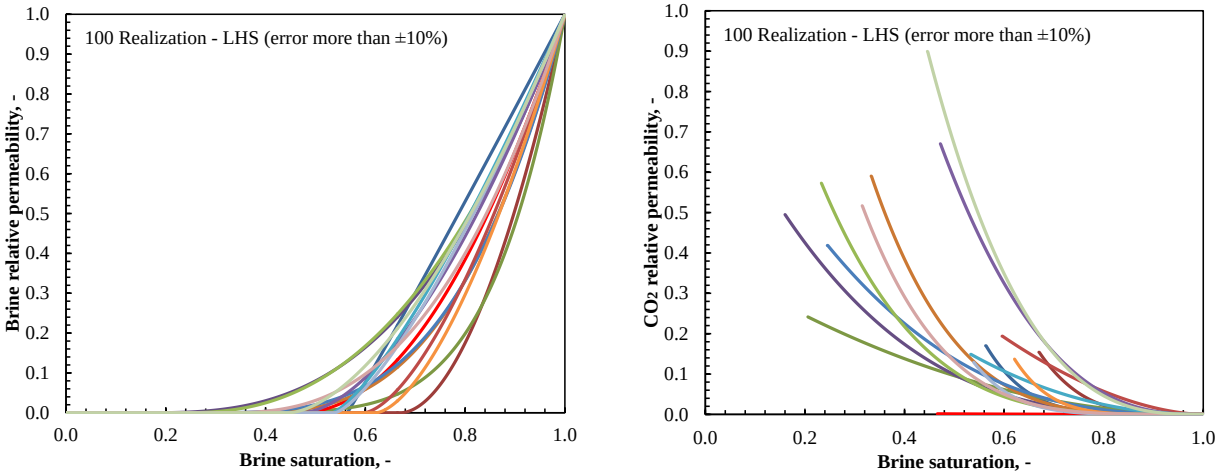

(a) Brine relative permeability (b) CO_2 relative permeability

Fig. 30 – Relative permeability curves providing more than ±10% error from regression line

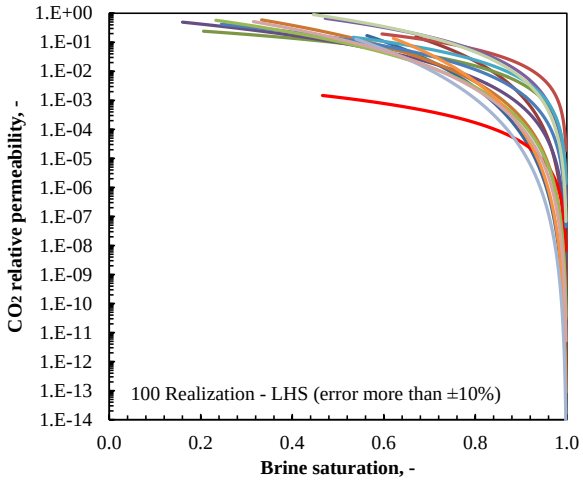

Fig. 31 – CO_2 relative permeability curves providing more than ±10% error in semi-log scale

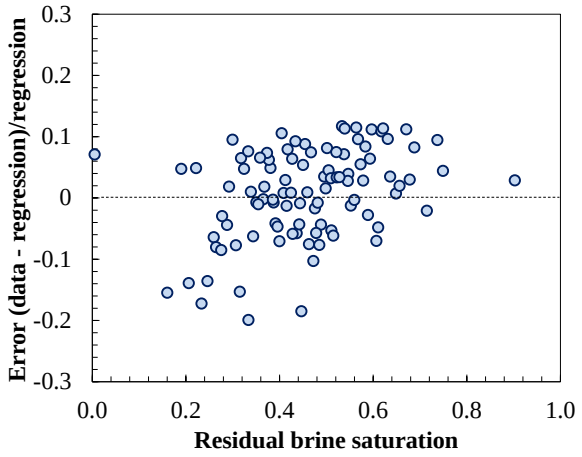

(a) Residual brine saturation

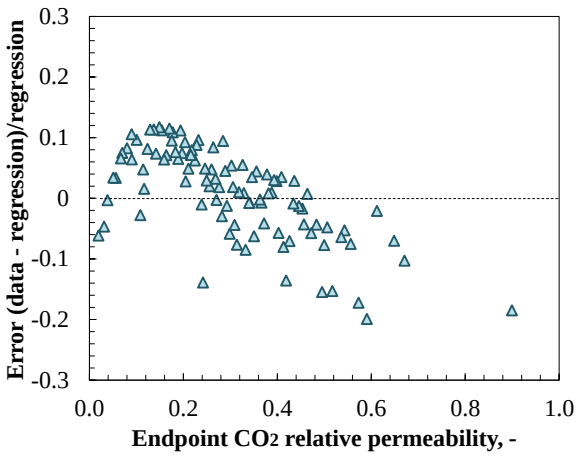

(b) Endpoint CO_2 relative permeability

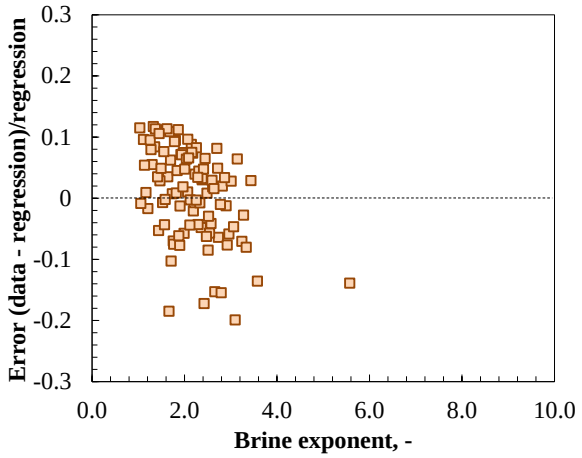

(c) Brine exponent

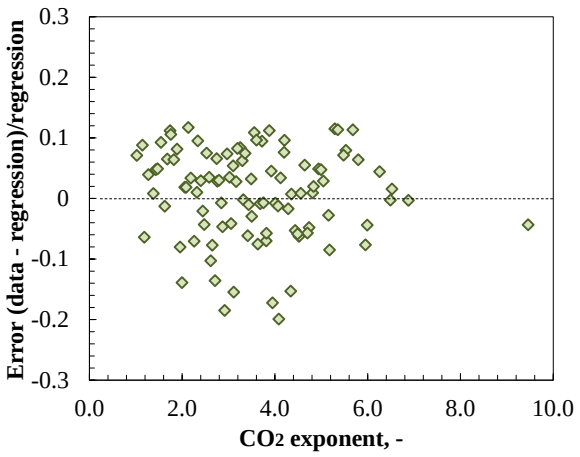

(d) CO_2 exponent

Fig. 32 – Relative error from the regression line with respect to each parameter (100 realizations)

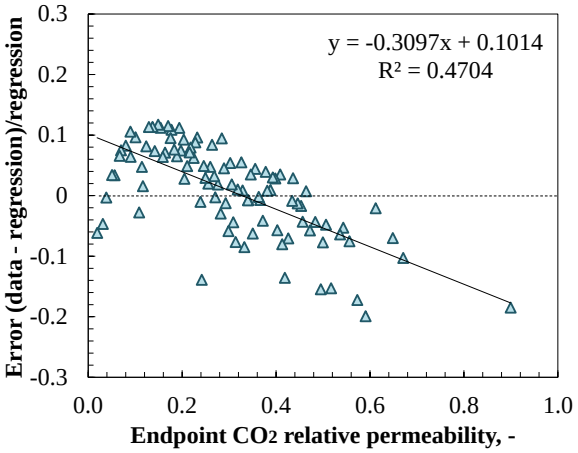

Fig. 33 – Relative error from the regression line to the endpoint CO2 relative permeability with weak negative relationship (100 realizations)

4.5 Implications for reduced order model (CO2-PENS)

The uncertainty quantification results by the Monte Carlo simulation shows the ±40% of the standard deviation to the mean value of total injected CO_2 amount. And also, the box plot in Fig. 23 reveals that the total injected CO_2 amount has wide range even if only the parameters of relative permeability model are changed. But, the Monte Carlo simulation and the regression analysis calibrated the conclusion given by the parameter sensitivity study that the total injected CO_2 amount is dominantly correlated by the endpoint CO_2 relative permeability. The relationship is described in the form of power equation, and the correlation coefficient is more than 0.99 ($R^2 = 0.9821$) against the target problem used in this report. The deviation from the regression line is thought to be mainly caused by the effects of the other parameters and their combination. The deviation or error from the regression line is at most ±20% (except the extremely small endpoint CO_2 relative permeability case).

Through these results and observations, in the reduced-order model, it is recommended that only the endpoint CO_2 relative permeability is considered as the variable in the Monte Carlo simulation for the uncertainty quantification in the relative permeability model (the maximum CO_2 effective permeability is the dominant parameter) while the other parameters are fixed using the mean value given by the experimental study of Bennion and Bachu (2008). Of course it is possible to include the all of these parameters in the analysis using such as the response surface method or multivariate polynomial regression (or nonlinear parametric regression method), but, as we presented in this work, the contribution by the others is considered to be limited (in this example the magnitude of the error is at most ±20%). In this report, we used the fixed absolute permeability under homogeneous and isotropic reservoir condition, and the effect of the absolute permeability should be considered in the reduced-order model. The maximum CO_2 effective permeability is the key factor for the risk analysis in the reduced-order model.

5 Conclusion

Relative permeability between brine and carbon dioxide (CO_2) is one of the crucial parameters on the injectivity, and to quantify the relative permeability relationship between brine and CO_2, several researchers conducted experiments. The work by Bennion and Bachu (2008) showed the valuable experimental data and the results of regression analysis to the extended Corey's model. At the first part of this report, we used the data given by Bennion and Bachu (2008) and run simulations with FEHM to find out the relationship between the CO_2 injectivity and the relative permeability curves. Though this study, it was found the injectivity has the strong relationship with the maximum CO_2 effective permeability. The results show the higher correlation coefficient comparing to only the absolute permeability or the endpoint CO_2 relative permeability.

Next, the parameter sensitivity study was performed to quantify the influence on the injectivity due to the change of the parameters in the relative permeability model. In this work, the data given by Bennion and Bachu (2008) was used to set the base case and the parameter variation range. In each simulation run, only one parameter value is changed with no change to the others and, by comparing the results to base case, the sensitivity of each parameter and the possible error range are quantified. The results confirmed the implication given by the preliminary study that the maximum CO_2 effective permeability has the dominant role in the determination of the injectivity. In addition, it was found the endpoint CO_2 permeability and the residual brine saturation has the positive relationship to the injectivity, and oppositely, the exponents of the brine and CO_2 has the negative relationship. These are confirmed though the physical interpretation of each parameter and the CO_2 plume contour plots after 4 years injection. And also, the possible error due to the variation of each parameter is quantified. Within the range between P10 to P90, the variation of the endpoint CO_2 relative permeability provides the ±60% difference while that of the other parameter provides at most ±10% difference in this specific problem.

Finally, for the calibration of the above results and uncertainty quantification, the Monte Carlo simulation study was performed. This study showed, as uncertainty quantification, the ±40% of the standard deviation to the mean value of total injected CO_2 amount and the total injected CO_2 amount has wide range even if only the parameters in the relative permeability model are changed. The regression analysis calibrated the implication that the total injected CO_2 amount is dominantly correlated by the endpoint CO_2 relative permeability. The uncertainty of the injectivity is mainly explained by the endpoint CO_2 relative permeability. The regression line is described in the form of power equation, and the correlation coefficient is more than 0.99 ($R^2 = 0.9821$). The deviation from the regression line is thought to be mainly caused by the effects of the other parameters and their combination. The deviation or error from the regression line is at most ±20%.

Through these results and observations, in the reduced-order model, it is recommended that the endpoint CO_2 relative permeability is considered as a variable in the Monte Carlo simulation for the uncertainty quantification in the relative permeability model while the other parameters are fixed using the mean value given by the experimental study of Bennion and Bachu (2008). In this report, we used the fixed absolute permeability under homogeneous and isotropic reservoir condition, and the effect of the absolute permeability should be considered in the reduced-order model. The maximum CO_2 effective permeability is the key factor for the risk analysis in the reduced-order model. This conclusion reminds readers of the importance of the work done by Levine (2011) in which they tried to measure the accurate endpoint CO2 relative permeability through the experiment.

Acknowledgement

This work is part of the Big Sky CO2-EOR/Storage Project that is supported by the U.S. Department of Energy and managed by the National Energy Technology Laboratory.

References

Azizi, E., & Cinar, Y. 2013. Approximate Analytical Solutions for CO_2 Injectivity Into Saline Formations. *SPE Reservoir Evaluation & Engineering*, **16** (2), 123-133.

Bachu, S. and Bennion, B. 2007. Effects of In Situ Conditions on Relative Permeability Characteristics of CO_2-brine System. *Environmental Geology.* DOI: 10.1007/s00254-007-0946-9

Bachu, S., and B. Bennion 2009. Interfacial tension between CO_2, freshwater, and brine in the range of pressure (2 to 27) mPa, temperature (20 to 125)C, and water salinity from (0 to 334 000) mg. l^{-1}, *J. Chem. Eng. Data*, 54, 765–775.

Bennion, B. and Bachu, S. 2005. Relative Permeability Characteristics for Supercritical CO_2 Displacing Water in a Variety of Potential Sequestration Zones in the Western Canada Sedimentary Basin. Paper SPE 95547 presented at the SPE Annual Technical Conference and Exhibition, Dallas, 9-12 October. DOI: 10.2118/95547-MS.

Bennion, D., & Bachu, S. 2006. The impact of interfacial tension and pore size distribution/capillary pressure character on CO_2 relative permeability at reservoir conditions in CO_2-brine systems. Paper SPE 99325 at the SPE/DOE Symposium on Improved Oil Recovery, Tulsa, 22-26 April

Bennion, D.B. and Bachu, S. 2008. Drainage and Imbibition Relative Permeability Relationships for Supercritical CO_2/Brine and H_2S/Brine Systems in Intergranular Sandstone, Carbonate, Shale, and Anhydrite Rocks. *SPE Res Eval & Eng* **11** (3): 487-496. http://dx.doi.org/10.2118/99326-PA

Chalbaud, C., Lombard, J. M., Martin, F., Robin, M., Bertin, H., & Egermann, P. 2007. Two Phase Flow Properties of Brine-CO_2 Systems in a Carbonate Core: Influence of Wettability on Pc and kr. Paper SPE 111420 presented at SPE/EAGE Reservoir Characterization and Simulation Conference, 28-31, October, Abu Dhabi, UAE.

Deng, H., Stauffer, P. H., Dai, Z., Jiao, Z., & Surdam, R. C. 2012. Simulation of industrial-scale CO_2 storage: Multi-scale heterogeneity and its impacts on storage capacity, injectivity and leakage. *International Journal of Greenhouse Gas Control*, **10**, 397-418.

Doughty, C. 2007. Modeling geologic storage of carbon dioxide: comparison of non-hysteretic and hysteretic characteristic curves. Energy Conversion and Management, **48** (6), 1768-1781.

Dria, D. E., Pope, G. A., & Sepehrnoori, K. 1993. Three-phase gas/oil/brine relative permeabilities measured under CO_2 flooding conditions. *SPE reservoir engineering*, **8** (2), 143-150.

Egermann, P., Chalbaud, C., Duquerroix, J., & Le Gallo, Y. 2006. An integrated approach to parameterize reservoir models for CO_2 injection in aquifers. Paper SPE 102308 presented at the SPE Annual Technical Conference and Exhibition, San Antonio, 24-27 September.

Juanes, R., Spiteri, E. J., Orr, F. M., & Blunt, M. J. 2006. Impact of relative permeability hysteresis on geological CO_2 storage. *Water Resources Research*, **42**(12).

Levine, J. 2011. Relative Permeability Experiments of Carbon Dioxide Displacing Brine and Their Implications for Carbon Sequestration. PhD Dissertation, Columbia University

Liu, N., Ghorpade, S., Harris, L., Li, L., Grigg, R., & Lee, R. 2010. The effect of pressure and temperature on brine-CO_2 relative permeability and IFT at reservoir conditions. Paper SPE139029 presented at the SPE Eastern Regional Meeting, October.

Müller, N. 2011. Supercritical CO_2-brine relative permeability experiments in reservoir rocks—Literature review and recommendations. *Transport in porous media*, **87** (2), 367-383.

Mohamed, I., & Nasr-El-Din, H. 2013. Fluid/Rock Interactions During CO_2 Sequestration in Deep Saline Carbonate Aquifers: Laboratory and Modeling Studies. *SPE Journal*, **18** (3), 468-485.

Perrin, J. C., Krause, M., Kuo, C. W., Miljkovic, L., Charoba, E., & Benson, S. M. 2009. Core-scale experimental study of relative permeability properties of CO_2 and brine in reservoir rocks. *Energy Procedia*, **1** (1), 3515-3522.

Pruess, K., García, J., Kovscek, T., Oldenburg, C., Rutqvist, J., Steefel, C., & Xu, T. 2002. Intercomparison of numerical simulation codes for geologic disposal of CO_2.

Stauffer P. H.; Viswanathan H. S.; Pawar R. J.; Klasky M. L.; Guthrie G. D. 2006. CO2-PENS a CO_2 sequestration system model supporting risk-based decisions. In Proceedings of the 16th International Conference on Computational Methods in Water Resources; Copenhagen, Denmark, June 19-22.

Stauffer, P. H., & Lu, Z. 2012. Quantifying transport uncertainty in unsaturated rock using Monte Carlo sampling of retention curves. *Vadose Zone Journal*, **11** (4).

Van Genuchten, M.Th. A Closed-Form Equation for Predicting the Hydraulic Conductivity of Unsaturated Soils, *Soil Sci. Soc. Am. J.*, Vol. 44, pp. 892 – 898, 1980.

Wyss, G. D., & Jorgensen, K. H. (1998). A user's guide to LHS: Sandia's Latin hypercube sampling software. SAND98-0210, Sandia National Laboratories, Albuquerque, NM.

Appendix

Calibration of the matched relative permeability curve with experimental data

Bennion and Bachu (2005) provided the experimental results for several rock samples. Using Eq. 3 and Eq. 4 with the results given by the regression analysis in Table 2, we performed the calibration of the results. Fig. A.1 shows the comparison plots of the data and the generated curves. According to the results, we found the values given by the Bennion and Bachu (2008) are reasonable except the brine exponential value in the case of Cooking Lake rock sample. In the paper, the value is originally 1.4, but we could not get the good match shown in Fig. A.1 (f). Then, we change the value to 3.1 to get the better match shown in the figure. This modified value is used in the Table 2.

Relative permeability curves given by Bennion and Bachu (2008) for the base case input

In Fig. A.2, the relative permeability curves generated by the Eq. 3 and Eq. 4 with the input data shown in Table 2 are summarized. Because we are mainly focusing on the drainage process, the relative permeability curves only for the drainage experiment results are shown. As shown in Fig. A.1, the experiment was terminated at the time when the brine saturation reached the residual brine saturation, and the relative permeability less than that value is not shown in the figure. As the input data for the FEHM, we set constant relative permeability less than the residual brine saturation.

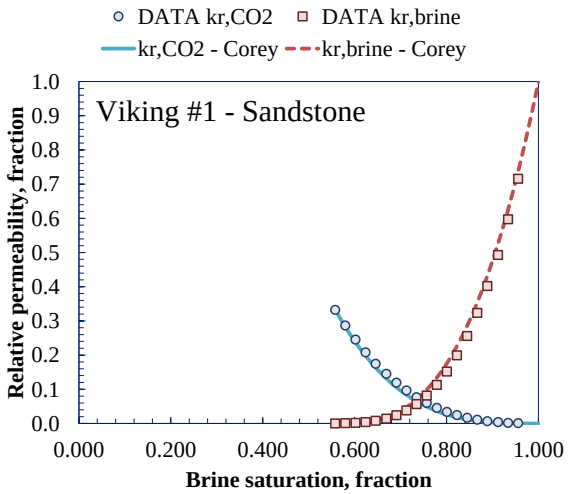

(a) Viking #1 – Sandstone

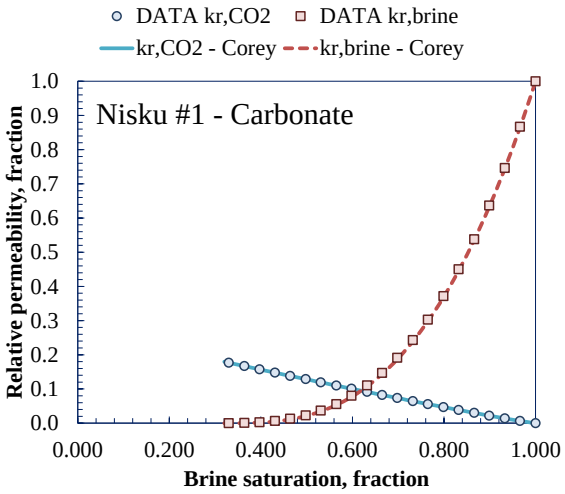

(d) Nisku #1 – Carbonate

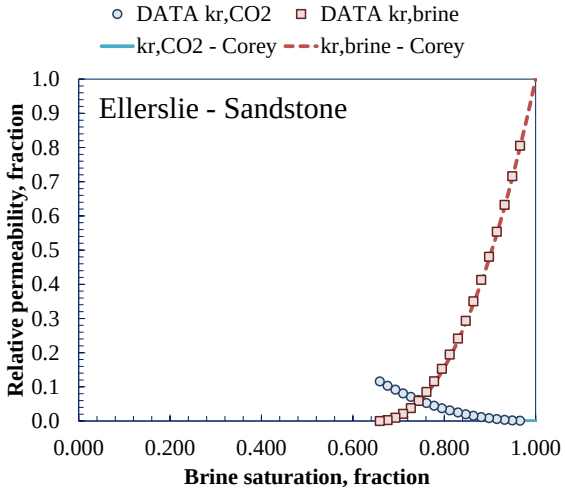

(b) Ellerslie - Sandstone

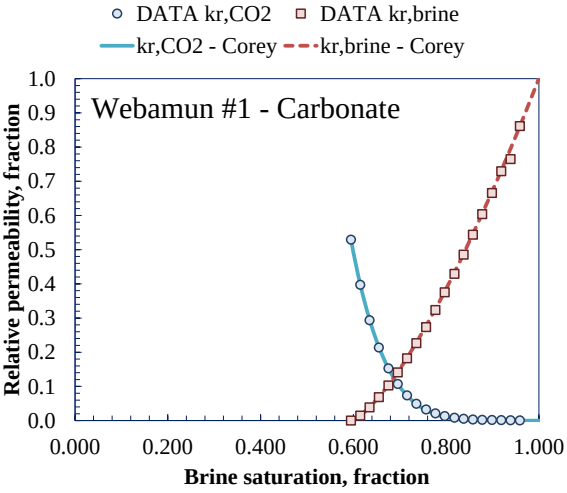

(e) Webamun #1 – Carbonate

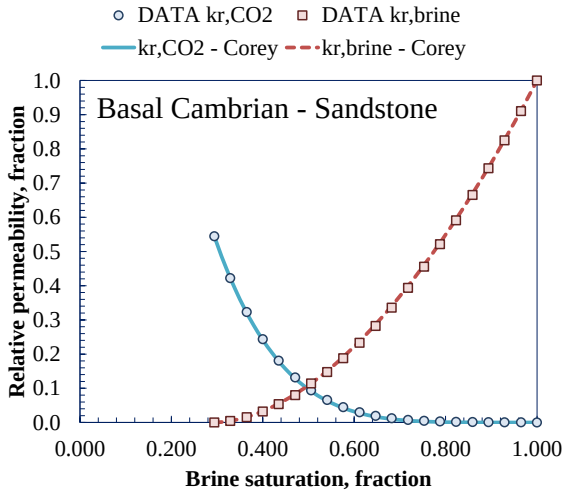

(c) Basal Cambrian – Sandstone

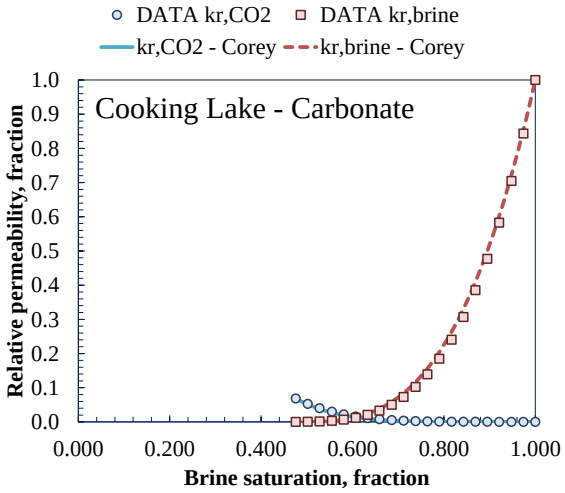

(f) Cooling Lake – Carbonate

Fig. A.1 - Calibration results (relative permeability curve and experimental data)

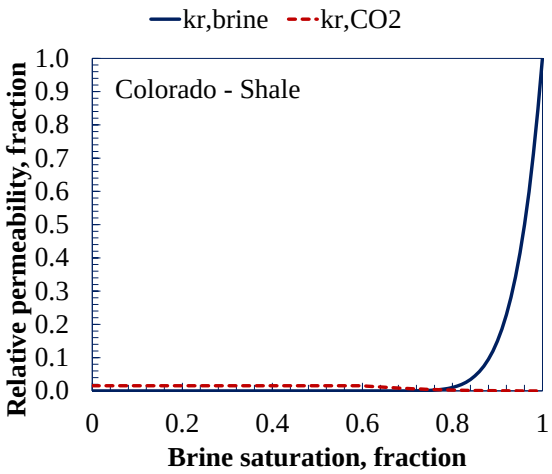

(a) Colorado – Shale

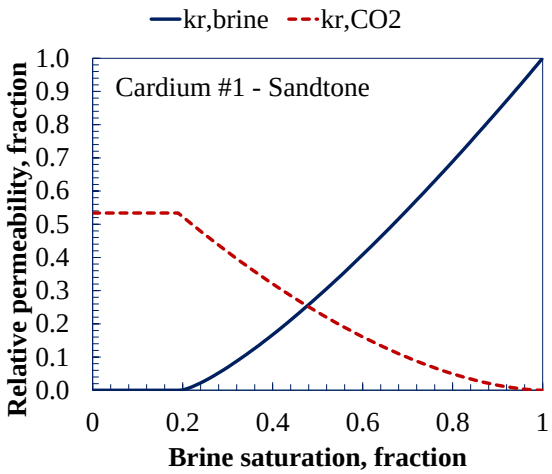

(b) Cardium #1 – Sandstone

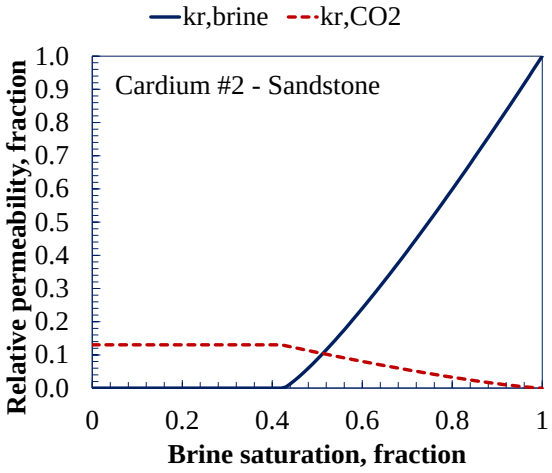

(c) Cardium #2 – Sandstone

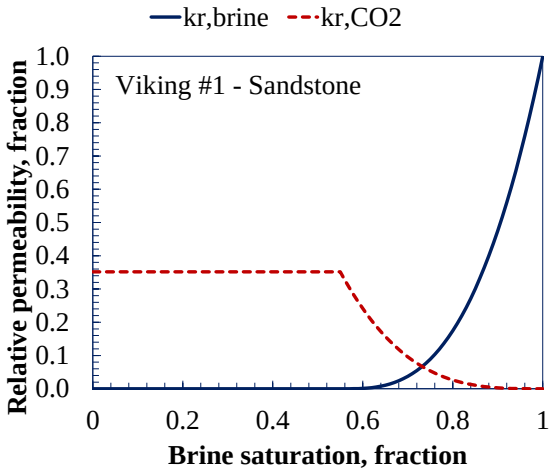

(d) Viking #1 – Sandstone

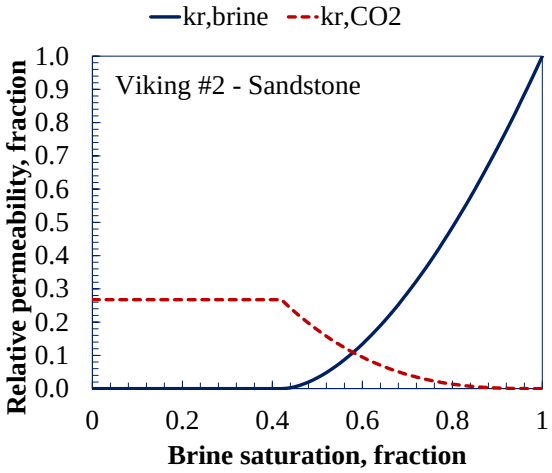

(e) Viking #2 – Sandstone

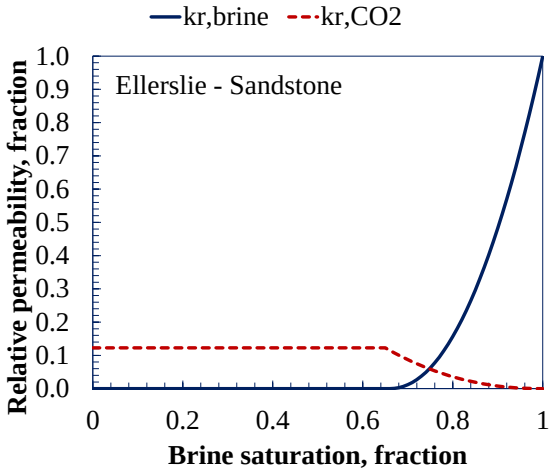

(f) Ellerslie – Sandstone

Fig. A.2 – Relative permeability curves for base case using the results by Bennion and Bachu (2008)

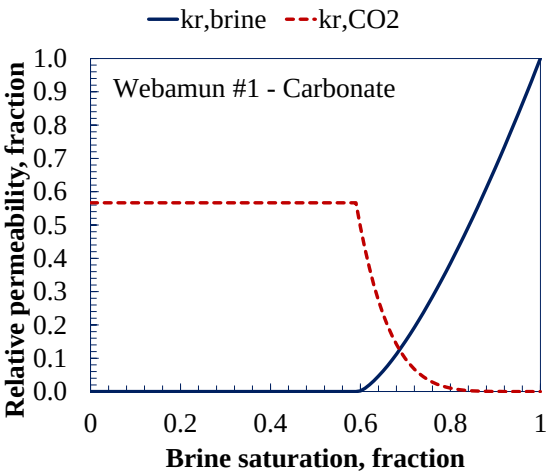

(g) Webamun #1 – Carbonate

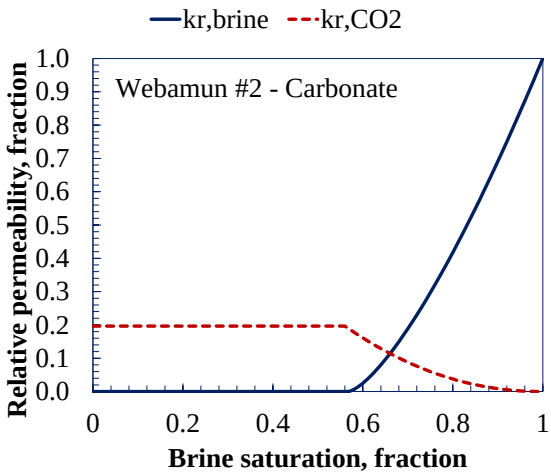

(h) Webamun #2 – Carbonate

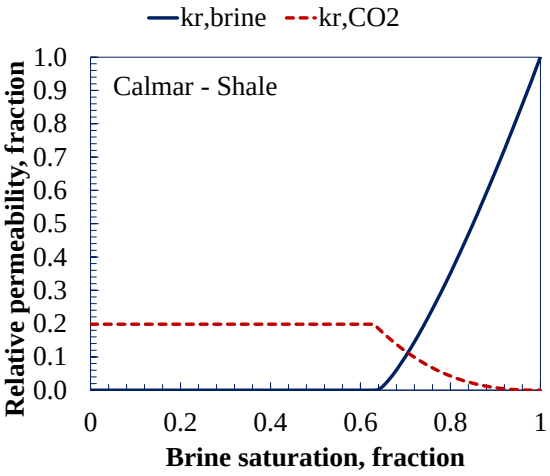

(i) Calmar – Shale

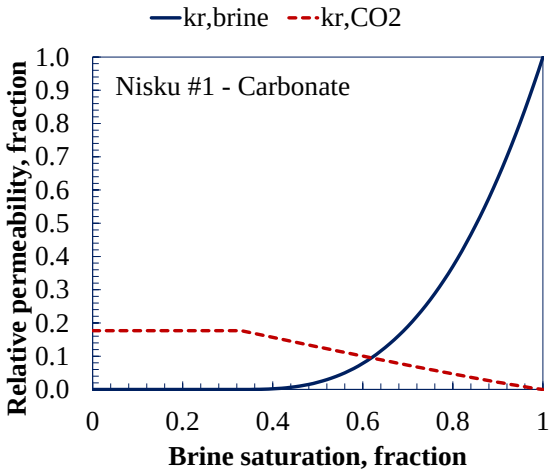

(j) Nisku #1 – Carbonate

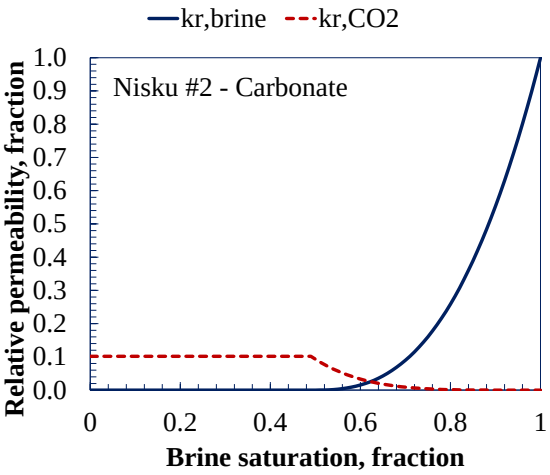

(k) Nisku #2 – Carbonate

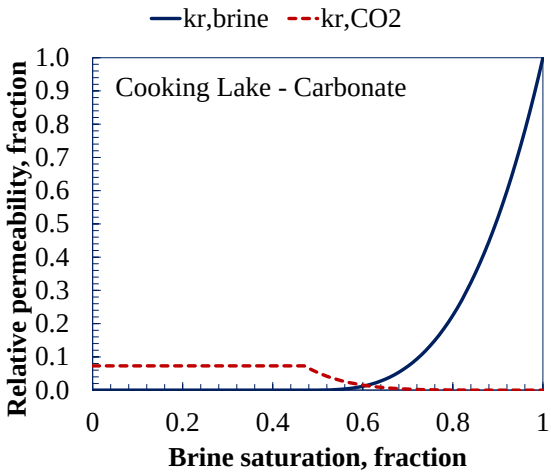

(l) Cooking Late – Carbonate

Fig. A.2 (continued)

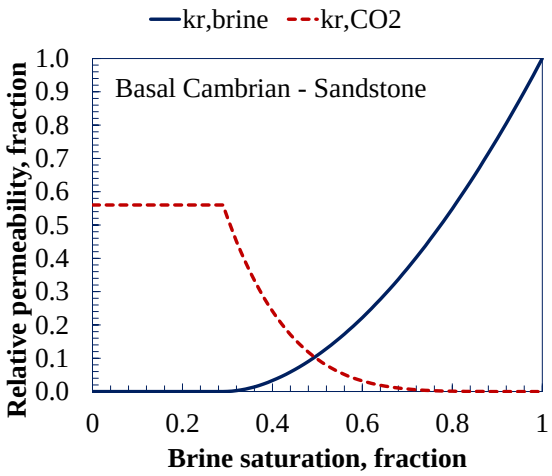

(m) Basal Cambrian – Sandstone

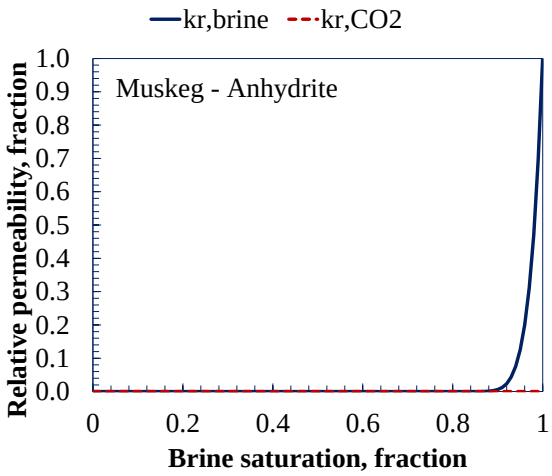

(n) Muskeg – Anhydrite

Fig. A.2 (continued)

Parameter values for Monte Carlo Simulation (given by LHS)

TABLE A.1 - VALUES FOR 25 REALIZATIONS

No.	$S_{r,b}$	n_{brine}	n_{CO2}	$k^0_{r,CO2}$	No.	$S_{r,b}$	n_{brine}	n_{CO2}	$k^0_{r,CO2}$
1	0.230	2.553	5.342	0.337	14	0.569	1.290	4.285	0.120
2	0.523	2.396	2.753	0.143	15	0.315	3.487	5.119	0.192
3	0.272	3.255	3.874	0.164	16	0.029	2.263	2.615	0.279
4	0.491	2.804	3.746	0.273	17	0.447	2.730	4.680	0.036
5	0.398	1.777	5.933	0.210	18	0.543	2.031	2.503	0.296
6	0.836	1.705	2.076	0.410	19	0.416	1.466	1.428	0.179
7	0.450	2.998	1.664	0.069	20	0.602	1.873	8.870	0.412
8	0.390	2.475	3.649	0.449	21	0.508	2.106	4.856	0.386
9	0.338	2.158	3.270	0.326	22	0.428	1.950	2.331	0.248
10	0.345	2.292	4.505	0.502	23	0.465	1.573	2.999	0.367
11	0.633	1.036	1.110	0.092	24	0.492	1.599	3.051	0.230
12	0.364	2.585	3.365	0.544	25	0.660	1.820	1.949	0.686
13	0.580	1.262	3.982	0.486					

TABLE A.2 - VALUES FOR 50 REALIZATIONS									
No.	$S_{r,b}$	n_{brine}	n_{CO2}	$k^0_{r,CO2}$	No.	$S_{r,b}$	n_{brine}	n_{CO2}	$k^0_{r,CO2}$
1	0.296	2.543	2.706	0.356	26	0.436	2.064	5.660	0.330
2	0.677	2.249	1.727	0.544	27	0.705	1.172	5.422	0.458
3	0.381	3.378	2.814	0.049	28	0.498	2.912	2.940	0.310
4	0.466	2.722	3.230	0.202	29	0.396	2.381	1.378	0.512
5	0.410	2.456	3.289	0.476	30	0.341	2.314	4.317	0.096
6	0.752	2.097	2.418	0.176	31	0.508	1.533	3.385	0.493
7	0.531	1.765	4.240	0.278	32	0.449	1.579	4.389	0.023
8	0.328	1.666	3.530	0.072	33	0.425	2.760	3.134	0.594
9	0.519	1.736	4.614	0.183	34	0.552	1.989	2.043	0.278
10	0.204	1.401	4.445	0.419	35	0.641	1.877	2.136	0.439
11	0.594	2.134	5.964	0.138	36	0.658	3.021	3.419	0.032
12	0.389	1.700	5.198	0.246	37	0.318	2.849	1.159	0.343
13	0.609	1.816	2.733	0.399	38	0.529	1.113	4.098	0.088
14	0.373	1.521	1.500	0.193	39	0.400	2.669	4.705	0.317
15	0.356	7.107	3.824	0.140	40	0.542	1.445	5.777	0.372
16	0.565	3.083	4.007	0.289	41	0.505	1.634	3.689	0.261
17	0.485	1.849	3.635	0.121	42	0.281	2.419	1.935	0.297
18	0.308	2.462	2.623	0.221	43	0.579	2.511	1.810	0.213
19	0.599	2.172	4.865	0.360	44	0.462	1.970	3.059	0.234
20	0.364	1.392	7.185	0.168	45	0.481	2.218	5.144	0.611
21	0.631	1.249	6.551	0.158	46	0.239	3.191	2.519	0.405
22	0.024	2.276	1.168	0.111	47	0.471	2.029	1.671	0.526
23	0.556	1.313	2.227	0.335	48	0.454	1.050	3.926	0.240
24	0.275	2.140	4.957	0.428	49	0.432	1.911	3.739	0.258
25	0.232	2.594	2.299	0.384	50	0.415	2.825	2.995	0.657

TABLE A.3 - VALUES FOR 100 REALIZATIONS

No.	$S_{r,b}$	n_{brine}	n_{CO2}	$k^0_{r,CO2}$	No.	$S_{r,b}$	n_{brine}	n_{CO2}	$k^0_{r,CO2}$
1	0.190	2.006	4.993	0.114	40	0.417	1.275	5.530	0.218
2	0.485	2.926	5.952	0.314	41	0.334	3.096	4.084	0.590
3	0.259	2.732	1.183	0.536	42	0.428	2.960	4.489	0.298
4	0.564	1.034	5.291	0.170	43	0.463	1.768	3.630	0.556
5	0.264	3.336	1.955	0.413	44	0.589	3.277	5.155	0.108
6	0.903	3.437	5.044	0.436	45	0.318	2.446	1.679	0.189
7	0.656	2.817	4.832	0.255	46	0.505	1.841	3.922	0.289
8	0.611	2.360	4.735	0.506	47	0.246	3.577	2.710	0.418
9	0.408	2.486	1.378	0.381	48	0.546	3.009	3.163	0.205
10	0.459	1.166	4.813	0.388	49	0.597	1.599	1.740	0.194
11	0.521	2.159	2.527	0.070	50	0.567	1.114	4.206	0.232
12	0.495	1.418	3.021	0.346	51	0.715	2.193	2.444	0.612
13	0.442	2.293	2.476	0.456	52	0.510	2.381	3.489	0.268
14	0.671	1.865	3.879	0.154	53	0.233	2.423	3.947	0.573
15	0.206	5.573	1.997	0.242	54	0.617	1.682	3.555	0.177
16	0.467	1.974	3.357	0.197	55	0.404	1.451	1.755	0.090
17	0.583	1.355	3.253	0.264	56	0.387	2.213	2.845	0.341
18	0.300	1.259	2.337	0.175	57	0.528	2.289	4.123	0.051
19	0.607	1.757	3.811	0.648	58	0.472	1.710	2.616	0.670
20	0.488	1.568	9.458	0.483	59	0.354	2.776	3.433	0.239
21	0.160	2.794	3.112	0.495	60	0.339	2.068	2.318	0.318
22	0.579	1.470	2.759	0.398	61	0.749	2.311	6.257	0.355
23	0.636	1.639	2.584	0.409	62	0.412	2.595	2.401	0.249
24	0.450	1.136	3.100	0.302	63	0.501	2.700	1.890	0.123
25	0.538	1.924	5.479	0.216	64	0.275	2.511	5.176	0.332
26	0.467	2.033	2.201	0.001	65	0.455	2.147	1.142	0.228
27	0.515	1.877	3.414	0.019	66	0.573	1.301	4.641	0.326
28	0.560	2.255	6.879	0.038	67	0.533	1.326	2.132	0.149
29	0.498	2.637	6.524	0.116	68	0.478	2.543	4.700	0.402
30	0.649	1.736	4.355	0.464	69	0.688	2.257	3.193	0.080
31	0.333	1.553	4.197	0.183	70	0.222	1.494	4.942	0.211
32	0.476	1.208	4.286	0.453	71	0.522	2.867	2.187	0.056
33	0.424	1.822	4.557	0.328	72	0.307	1.896	2.649	0.500
34	0.396	3.061	2.872	0.031	73	0.373	2.177	2.968	0.142
35	0.427	2.042	5.797	0.159	74	0.391	2.573	3.054	0.372
36	0.277	2.520	3.499	0.282	75	0.481	2.332	4.006	0.340
37	0.386	2.123	6.489	0.270	76	0.593	3.143	1.819	0.090
38	0.350	1.526	3.753	0.366	77	0.444	1.055	3.680	0.434
39	0.547	2.229	1.272	0.378	78	0.324	2.413	1.431	0.260

TABLE A.3 - VALUES FOR 100 REALIZATIONS (CONTINUTED)									
No.	$S_{r,b}$	n_{brine}	n_{CO2}	$k^0_{r,CO2}$	No.	$S_{r,b}$	n_{brine}	n_{CO2}	$k^0_{r,CO2}$
79	0.621	1.621	5.356	0.137	90	0.005	1.939	1.021	0.163
80	0.400	3.240	2.258	0.426	91	0.631	2.070	3.601	0.100
81	0.358	2.089	2.744	0.067	92	0.678	2.382	2.794	0.393
82	0.434	1.783	1.543	0.203	93	0.737	1.803	3.722	0.284
83	0.381	2.718	1.471	0.246	94	0.539	1.371	5.679	0.129
84	0.292	1.968	2.056	0.306	95	0.552	2.899	4.067	0.292
85	0.415	1.904	1.624	0.446	96	0.343	2.475	4.519	0.350
86	0.377	1.698	3.297	0.224	97	0.511	1.440	4.437	0.543
87	0.436	1.992	3.817	0.472	98	0.365	1.582	3.319	0.363
88	0.288	2.118	5.989	0.309	99	0.315	2.655	4.341	0.517
89	0.367	2.610	2.085	0.276	100	0.447	1.666	2.917	0.899